

1 **Reactive bromine chemistry in Mt Etna's volcanic plume: the**  
2 **influence of total Br, high temperature processing, aerosol loading**  
3 **and plume-air mixing**

4

5 **T. J. Roberts<sup>1</sup>, R. S. Martin<sup>2</sup>, and L. Jourdain<sup>1</sup>**

6

7 [1] {LPC2E, UMR 7328, CNRS-Université d'Orléans, 3A Avenue de la Recherche  
8 Scientifique, 45071 Orleans, Cedex 2, France}

9 [2] {Department of Geography, University of Cambridge, Downing Place, CB2 3EN, UK}

10

11 Correspondence to: T. J. Roberts (Tjarda.Roberts@cnsr-orleans.fr)

12

## 1 **Abstract**

2 Volcanic emissions present a source of reactive halogens to the troposphere, through rapid  
3 plume chemistry that converts the emitted HBr to more reactive forms such as BrO. The  
4 nature of this process is poorly quantified, yet is of interest to understand volcanic impacts on  
5 the troposphere, and infer volcanic activity from volcanic gas measurements (i.e. BrO/SO<sub>2</sub>  
6 ratios). Recent observations from Etna report an initial increase and subsequent plateau or  
7 decline in BrO/SO<sub>2</sub> ratios with distance downwind.

8 We present daytime *PlumeChem* model simulations that reproduce and explain the reported  
9 trend in BrO/SO<sub>2</sub> at Etna including the initial rise and subsequent plateau. Suites of model  
10 simulations also investigate the influences of volcanic aerosol loading, bromine emission, and  
11 plume-air mixing rate on the downwind plume chemistry. Emitted volcanic HBr is converted  
12 into reactive bromine by autocatalytic bromine chemistry cycles whose onset is accelerated  
13 by the model high-temperature initialisation. These rapid chemistry cycles also impact the  
14 reactive bromine speciation through inter-conversion of Br, Br<sub>2</sub>, BrO, BrONO<sub>2</sub>, BrCl, HOBr.

15 We predict a new evolution of Br-speciation in the plume. BrO, Br<sub>2</sub>, Br and HBr are the main  
16 plume species near downwind whilst BrO and HOBr are present further downwind (where  
17 BrONO<sub>2</sub> and BrCl also make up a minor fraction). BrNO<sub>2</sub> is predicted to be only a relatively  
18 minor plume component.

19 The initial rise in BrO/SO<sub>2</sub> occurs as ozone is entrained into the plume whose reaction with  
20 Br promotes net formation of BrO. Aerosol has a modest impact on BrO/SO<sub>2</sub> near-downwind  
21 (< ~6 km, ~10 min) at the relatively high loadings considered. The subsequent decline in  
22 BrO/SO<sub>2</sub> occurs as entrainment of oxidants HO<sub>2</sub> and NO<sub>2</sub> promotes net formation of HOBr  
23 and BrONO<sub>2</sub>, whilst the plume dispersion dilutes volcanic aerosol so slows the heterogeneous  
24 loss rates of these species. A higher volcanic aerosol loading enhances BrO/SO<sub>2</sub> in the (>  
25 6km) downwind plume.

26 Simulations assuming low/medium and high Etna bromine emissions scenarios show the  
27 bromine emission has a greater influence on BrO/SO<sub>2</sub> further downwind and a modest impact  
28 near downwind, and show either complete or partial conversion of HBr into reactive bromine,  
29 respectively, yielding BrO contents that reach up to ~50% or ~20% of total bromine (over a  
30 timescale of a few 10's of minutes).

1 Plume-air mixing non-linearly impacts the downwind BrO/SO<sub>2</sub>, as shown by simulations  
2 with varying plume dispersion, wind-speed and volcanic emission flux. Greater volcanic  
3 emission flux leads to lower BrO/SO<sub>2</sub> ratios near downwind, but also delays the subsequent  
4 decline in BrO/SO<sub>2</sub>, thus yields higher BrO/SO<sub>2</sub> ratios further downwind. We highlight the  
5 important role of plume chemistry models for the interpretation of observed changes in  
6 BrO/SO<sub>2</sub> during/prior to volcanic eruptions, as well as for quantifying volcanic plume  
7 impacts on atmospheric chemistry. Simulated plume impacts include ozone, HO<sub>x</sub> and NO<sub>x</sub>  
8 depletion, the latter converted into HNO<sub>3</sub>. Partial recovery of ozone occurs with distance  
9 downwind, although cumulative ozone loss is ongoing over the three hour simulations.  
10

## 1 1. Introduction

2 The discovery of volcanic BrO (Bobrowski et al., 2003), and its subsequent observation in  
3 many volcanic plumes globally (e.g. Oppenheimer et al., 2006, Bobrowski et al., 2007a;b,  
4 Kern et al., 2009, Bani et al., 2009, Louban et al., 2009, Theys et al., 2009, Boichu et al.,  
5 2011, Heue et al., 2011, Bobrowski and Giuffrida 2012, Rix et al., 2012, Hörmann et al.,  
6 2013, Kelly et al., 2013, Lübcke et al., 2013), demonstrates the reactivity of volcanic halogen  
7 emissions in the troposphere. Volcanoes release H<sub>2</sub>O, CO<sub>2</sub> and SO<sub>2</sub>, but also a range of  
8 hydrogen halides to the atmosphere including HF, HCl, and HBr (in descending order of  
9 abundance in the emission, see e.g. Aiuppa et al. 2005). HF is too strong an acid for reactive  
10 halogen cycling, but for HBr and HCl, observational evidence shows these are not simply just  
11 washed-out from the atmosphere, but can undergo transformation into reactive halogen  
12 species.

13 Notably, DOAS (Differential Optical Absorption Spectroscopy) measurements show BrO  
14 forms at 100's pmol/mol to nmol/mol mixing ratios just minutes downwind, an order of  
15 magnitude higher than that found in the Arctic, where BrO episodes of up to 10's pmol/mol  
16 cause significant ozone depletion and mercury deposition events (Simpson et al., 2007).  
17 Additionally, there is potential to use long-term BrO monitoring at volcanoes as an indicator  
18 of volcanic activity (Bobrowski and Giuffrida, 2012). Thus there is strong interest in  
19 developing models to simulate the formation of reactive bromine (and chlorine) in volcanic  
20 plumes, and to predict the downwind impacts from both quiescently degassing volcanoes and  
21 episodic eruptions to the troposphere. Studies to date usually use equilibrium models to  
22 predict the high-temperature chemistry of the near vent plume, which is then used to initialise  
23 kinetic atmospheric chemistry models of the downwind reactive halogen chemistry  
24 (Bobrowski et al., 2007a, Roberts et al., 2009, von Glasow 2010, Kelly et al., 2013). See von  
25 Glasow et al. (2009) for an overview.

26 This study uses a purpose-built kinetic model, *PlumeChem* (Roberts et al., 2009), to  
27 investigate the volcanic plume reactive halogen chemistry, focusing here on bromine in a  
28 case study for Mt Etna. We include a revised methodology (Martin et al., 2009) for  
29 equilibrium calculations used to represent the near-vent high-temperature chemistry, and  
30 discuss uncertainties in the use of thermodynamic equilibrium models. Below, we outline the  
31 progression of recent research on using equilibrium models for high-temperature near-vent  
32 plume chemistry and the development of kinetic models for volcanic plume reactive halogen

1 (BrO) chemistry. We then describe the new findings of this study specifically regarding the  
2 in-plume reactive bromine evolution presented by the model, and to highlight uncertainties in  
3 model high-temperature initialisation and the influence of total bromine, aerosol and plume-  
4 air mixing on the plume chemistry.

5

## 6 **1.1 Application of the HSC Equilibrium model to the near-vent plume**

7 HSC is a commercially available model (Outokumpo, Finland) that predicts the  
8 thermodynamic equilibrium composition of a gas mixture at a defined temperature, pressure  
9 and chemical composition. Such models are used to represent the composition of the near-  
10 vent volcano plume (e.g. Gerlach, 2004, Martin et al., 2006), predicting a vast array ( $\geq 100$ ) of  
11 chemical species. An overview of the input and outputs to HSC is provided in Table 1. The  
12 chemical composition of the mixture is determined by combining magmatic (comprising of  
13 H<sub>2</sub>O, CO<sub>2</sub>, CO, SO<sub>2</sub>, H<sub>2</sub>S, H<sub>2</sub>, HF, HCl, HBr, HI, Hg, typically at around 800-1100°C) and air  
14 (N<sub>2</sub>, O<sub>2</sub>, Ar, typically around 0-20°C) components. The magmatic gas composition varies  
15 between volcanoes and may be estimated from crater-rim measurements. It is also possible to  
16 predict the abundance of gases that are missing from measurements as the magmatic gas  
17 H<sub>2</sub>O-H<sub>2</sub>, CO<sub>2</sub>-CO, SO<sub>2</sub>-H<sub>2</sub>S equilibria are functions of oxygen fugacity, pressure of degassing  
18 and temperature (e.g. Giggenbach, 1987). The resulting HSC output composition depends  
19 critically on the assumed ratio of air to magmatic gases in the near-vent plume,  $V_A:V_M$ .  
20 However, this ratio is poorly defined, an issue we examine further in this study.

21 The HSC output is then used to initialise low-temperature kinetic models (such as  
22 *PlumeChem*, Roberts et al., 2009, Kelly et al., 2013, *MISTRA*, Bobrowski et al., 2007a, von  
23 Glasow, 2010) of the volcanic plume reactive halogen chemistry including formation of BrO.  
24 These models show that elevated radicals in the HSC output accelerate the onset of  
25 autocatalytic BrO chemistry, leading to very rapid BrO formation. BrO formation occurs  
26 more slowly in kinetic models that are not initialised with high temperature chemistry. For  
27 the interest of atmospheric modellers, we simplify the complex HSC output ( $\geq 100$  species) in  
28 Table 1, following Roberts et al. (2009) who identified impacts of HO<sub>x</sub>, NO<sub>x</sub>, Br<sub>x</sub> and Cl<sub>x</sub> on  
29 the downwind plume halogen chemistry. The key species are further identified to be OH, NO,  
30 Br, Cl and Cl<sub>2</sub>, noting NO<sub>2</sub>  $\ll$  NO and HO<sub>2</sub>  $\ll$  OH, Br<sub>2</sub>  $\ll$  Br in the HSC output. These  
31 species act to accelerate autocatalytic reactive bromine formation (see Figure 4 of Roberts et  
32 al., 2009). High-temperature near-vent formation of SO<sub>3</sub> (a precursor to H<sub>2</sub>SO<sub>4</sub>) also

1 influences the volcanic plume halogen chemistry by providing a source of aerosol surface  
2 area.

3 However, the thermodynamic assumption behind equilibrium models such as HSC may not  
4 always be appropriate for volcanic plume applications: Martin et al. (2009) noted that the  
5 near-complete re-equilibration (i.e., oxidation) of H<sub>2</sub>S within HSC is in disagreement with the  
6 widespread observed presence of H<sub>2</sub>S in volcanic plumes (exception: Erebus), and suggested  
7 a revised operation of HSC in which H<sub>2</sub>S is removed prior to re-equilibration. Furthermore,  
8 recent measurements confirming volcanic H<sub>2</sub> (Aiuppa et al., 2011, Roberts et al., 2012)  
9 indicate this argument also applies to H<sub>2</sub>, as well as CO (although CO is typically present in  
10 low concentrations, with some exceptions e.g. Mt. Erebus. See e.g. Gerlach, 2004 for various  
11 collated emission compositions. Uncertainties and limitations in the use of HSC to represent  
12 the near-vent plume composition are discussed further in this study in the context of  
13 downwind BrO chemistry.

14

## 15 **1.2 Kinetic models of downwind volcanic plume reactive halogen chemistry**

16 Atmospheric chemistry models have been developed in an effort to simulate the reactive  
17 halogen chemistry of volcanic plumes, explain observed BrO formation and predict impacts  
18 of reactive volcanic halogens on atmospheric chemistry. To date, two models: *MISTRA* (that  
19 simulates an advected column of air, Bobrowski et al., 2007a) and *PlumeChem* (in an  
20 expanding box or multi-grid box modes, Roberts et al., 2009) have been developed for this  
21 purpose. Initialisation of these models includes the high-temperature chemistry of the near-  
22 vent plume, as represented by HSC. Calculations by Oppenheimer et al. (2006) showed BrO  
23 formation to be too slow if high-temperature near-vent radical formation is ignored.  
24 Bobrowski et al. (2007a) performed the first *MISTRA* kinetic model simulations of volcanic  
25 plume reactive halogen chemistry, using a model initialised with HSC at V<sub>A</sub>:V<sub>M</sub> of 0:100,  
26 15:85, 40:60 finding the 40:60 simulation yielded highest downwind BrO/SO<sub>2</sub>. Roberts et al.,  
27 (2009) queried the use of such high V<sub>A</sub>:V<sub>M</sub> of 40:60 which yields rather high SO<sub>3</sub>:SO<sub>2</sub> ratios,  
28 that implies volcanic sulfate emissions would exceed volcanic SO<sub>2</sub>. Roberts et al. (2009)  
29 presented model simulations initialised with HSC at V<sub>A</sub>:V<sub>M</sub> of 10:90 that reproduced the  
30 rapid formation of BrO/SO<sub>2</sub> at a range of Arc (subduction zone) volcanoes for the first time  
31 (including Etna, Soufriere Hills, Villarrica), and suggested the higher BrO/SO<sub>2</sub> observed in  
32 the Soufriere Hills volcano plume may be fundamentally due to higher Br/S in the emission.

1 A model study by von Glasow (2010) with simulations initialised at  $V_A:V_M$  of 15:85  
2 demonstrated good agreement to both reported column abundances of  $\text{SO}_2$  and  $\text{BrO}/\text{SO}_2$   
3 ratios downwind of Etna.

4 All of the abovementioned simulations (Bobrowski et al., 2007a, Roberts et al., 2009, von  
5 Glasow 2010) predict substantial in-plume depletion of oxidants, including ozone, although  
6 to varying extents, and predict contrasting plume halogen evolution. Roberts et al., (2009)  
7 also demonstrated conversion of  $\text{NO}_x$  into nitric acid via  $\text{BrONO}_2$ , and proposed this  
8 mechanism to explain reported elevated  $\text{HNO}_3$  in volcano plumes. Von Glasow (2010)  
9 simulated the impacts of volcanic reactive halogen chemistry on mercury speciation  
10 predicting significant conversion to  $\text{Hg}^{\text{II}}$  in the plume.

11 A number of observations of ozone abundance in volcanic plumes have recently been  
12 reported: Vance et al. (2010) observed ozone depletion in the Eyjafjallajökull plume, and at  
13 ground-level on Etna's flanks (by passive sampling). Schumann et al. (2012) presented  
14 multiple measurements of the downwind plume of Eyjafjallajökull that observed ozone  
15 depletion to variable degrees. There exist also observations of depleted ozone in Mt St  
16 Helen's plume (Hobbs et al., 1982) that are now believed to be likely due to BrO chemistry.  
17 Ozone depletion of up to ~35 % was reported in an aircraft study of Mt Erebus plume in  
18 Antarctica (Oppenheimer et al., 2010), where BrO has also been observed (Boichu et al.,  
19 2011). A systematic instrumented aircraft investigation of ozone depletion in a volcano  
20 plume (where emissions are also quantified) is presented by Kelly et al. (2013), and  
21 compared to *PlumeChem* model simulations over 2 hours of plume evolution, finding good  
22 spatial agreement in the modelled and observed ozone mixing ratios. At higher altitudes,  
23 ozone depletion in a volcanic plume is reported in the UTLS (upper troposphere, lower  
24 stratosphere) region observed by Rose et al. (2006), and investigated and attributed to  
25 reactive halogen chemistry by Millard et al. (2006).

26 However, ozone depletion has not been universally observed: Baker et al. (2010) did not  
27 detect an ozone depletion signal relative to the (somewhat variable) background level during  
28 an aircraft transect through Eyjafjallajökull plume. An instrumented aircraft study found no  
29 evidence for  $\text{O}_3$  depletion in the plume of Nevado del Huila (Colombia) and found ozone  
30 levels 70-80 % of ambient in the plume of Tungurahua, (Ecuador), which could not be  
31 conclusively attributed to BrO chemistry (Carn et al., 2011).

1 A number of modelling discrepancies also exist. For example, the model studies of Roberts et  
2 al. (2009), von Glasow (2010), and Kelly et al. (2013), predict contrasting Br-speciation  
3 and contrast in predicted impacts on ozone and other oxidants. These may reflect differences  
4 in the model representations and modelling uncertainties or demonstrate volcano-specific  
5 differences in the plume chemistry. Navigating the vast model parameter space of volcanic  
6 plume chemistry is challenging due to the non-linear controls on the plume chemistry of  
7 multiple inter-dependent parameters including volcanic aerosol, rate of horizontal dispersion,  
8 rate of vertical dispersion, wind-speed, volcanic gas flux, bromine in the emission, and high-  
9 temperature radical formation. Limited observational datasets are available to compare to the  
10 models, and the available data do not fully constrain the high- and low-temperature plume  
11 chemistry. To provide further insight, this study presents new *PlumeChem* model simulations  
12 to compare to recently reported trends in BrO/SO<sub>2</sub> ratios, and illustrates several of the major  
13 controls and uncertainties in the reactive halogen chemistry of volcanic plumes.

14



## 1 **2. Methods**

### 2 **2.1 HSC: equilibrium modelling of near-vent plume chemistry**

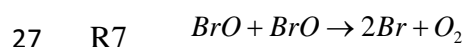
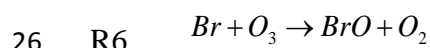
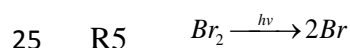
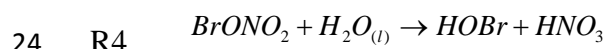
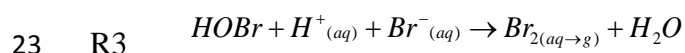
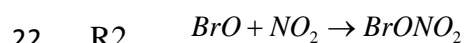
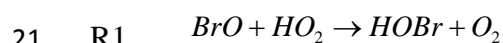
3 The use of HSC for calculating the composition of the near-vent plume is described by  
4 Gerlach (2004) and Martin et al. (2006). This study uses HSC thermodynamic model version  
5 7.1, and applying the modifications which were proposed by Martin et al. (2009). A simple  
6 background atmosphere of N<sub>2</sub> (78 %), O<sub>2</sub> (21 %) and Ar (1%) is assumed for the HSC  
7 calculations. The magmatic composition used for Etna follows that of Bagnato et al. (2007),  
8 with gas mixing ratios for H<sub>2</sub>O, CO<sub>2</sub>, SO<sub>2</sub>, H<sub>2</sub>, HCl, H<sub>2</sub>S, CO, of 0.86,  $9.6 \cdot 10^{-2}$ ,  $2.9 \cdot 10^{-2}$ ,  $5 \cdot 10^{-3}$ ,  
9  $1.4 \cdot 10^{-2}$ ,  $1.5 \cdot 10^{-3}$  and  $3.5 \cdot 10^{-4}$  respectively. Hg and CO are excluded for the purposes of this  
10 study due to their low abundances in the volcanic emission. The bromine content as HBr, was  
11 set to be either medium, high or low: ‘Medium’ bromine (molar mixing ratio of  $2.16 \times 10^{-5}$ ,  
12 equivalent to a total bromine to SO<sub>2</sub> ratio (Br<sub>tot</sub>/SO<sub>2</sub>) in the emission of  $7.4 \cdot 10^{-4}$ ) corresponds  
13 to the average Br/S molar ratio at Etna NEC crater determined from filter-pack measurements  
14 over 2004, Aiuppa et al. (2005). ‘High’ bromine (mixing ratio of  $7.03 \times 10^{-5}$ , equivalent to  
15 Br<sub>tot</sub>/SO<sub>2</sub> in the emission of  $2.4 \cdot 10^{-3}$ ) corresponds to that assumed in a previous model study  
16 of Etna (von Glasow, 2010), and is in the upper range (within one standard deviation) of the  
17 observations of Aiuppa et al. (2005). Simulations are also performed at a ‘lower’ Br<sub>tot</sub>/SO<sub>2</sub> =  
18  $4.8 \cdot 10^{-4}$  which corresponds to a filterpack Br/S measurement at Voragine crater reported by  
19 Oppenheimer et al. (2006). These are summarized in Table 2.

20 The magmatic temperature is set to 1050 °C in order to match that prescribed by von Glasow  
21 (2010), although we note Metrich and Rutherford (1998) estimated Etna magmatic  
22 temperature to be 1100°C. For the near-vent plume mixture input to HSC, ambient air  
23 temperature was set to 20°C. This is somewhat high considering Etna’s elevation (3 km), but  
24 this has a minor influence on the HSC output (especially considering 50 °C difference in the  
25 magmatic temperature estimates outlined above). For the actual *PlumeChem* atmospheric  
26 chemistry model runs, the atmospheric temperature was a more realistic 285 K. The  
27 equilibrium composition was calculated for standard operation of HSC (in which H<sub>2</sub> and H<sub>2</sub>S  
28 are allowed to re-equilibrate) and in a revised (Martin et al., 2009) operation of HSC (in  
29 which H<sub>2</sub> and H<sub>2</sub>S are replaced by inert Ar such that they do not re-equilibrate). The HSC  
30 calculations were performed over 16 different V<sub>A</sub>:V<sub>M</sub> ranging from 0:100 to 15:85.

### 31 **2.2 *PlumeChem*: kinetic model of downwind BrO chemistry**

1 The *PlumeChem* model simulates the reactive halogen chemistry of volcanic plume, as  
 2 described by Roberts et al. (2009). It can be run in single-box (Roberts et al., 2009) or multi-  
 3 box (Kelly et al. 2013) modes. Here we used the single-box that expands as a background  
 4 atmosphere is entrained into it, representing dispersion of the plume as it is advected  
 5 downwind. *PlumeChem* includes a background atmospheric chemistry scheme and bromine  
 6 and chlorine reactive halogen chemistry, including photolysis, gas-phase and heterogeneous  
 7 (gas-aerosol) phase reactions. Autocatalytic formation of BrO occurs through cycles  
 8 involving reaction of BrO with oxidants, ( $\text{HO}_2$ ,  $\text{NO}_2$ ), (R1,2), aerosol-phase heterogeneous  
 9 chemistry (R3,4) to release a halogen dimer, whose photolysis generates two halogen radicals  
 10 (R5), which may react with ozone (R6) to form BrO. The heterogeneous reactive uptake of  
 11 HOBr and  $\text{BrONO}_2$  on volcanic aerosol are thus key drivers of reactive halogen formation.  
 12 Within the volcanic aerosol, aqueous-phase equilibria (Wang et al. 1994) control the nature  
 13 of the product, which is  $\text{Br}_2$  for a typical volcanic plume composition, thereby enabling  
 14 autocatalytic formation of reactive bromine. Once aerosol  $\text{Br}^-_{(\text{aq})}$  becomes depleted (as  
 15 consequence of the BrO formation cycles), BrCl becomes a significant product from the  
 16 heterogeneous reactions (R3,R4), leading to non-autocatalytic formation of reactive chlorine.  
 17 Repeated cycling around R1-R6 can cause substantial ozone loss (orders of magnitude greater  
 18 than the BrO mixing ratio). Repeated cycling between BrO and Br (R6, R7) further enhances  
 19 ozone loss in concentrated plume environments.

20



28

1 The background atmosphere chemistry scheme used here is identical to that of Roberts et al.  
2 (2009), assuming a somewhat polluted atmosphere. For the model simulations initialised  
3 around midday, background ozone is ~60 nmol/mol, NO<sub>x</sub> and HO<sub>x</sub> are around 0.17 nmol/mol  
4 and 30 pmol/mol respectively, with an ambient temperature of 285 K and 60% relative  
5 humidity (RH). Plume dispersion is defined according to Pasquill-Gifford dispersion schemes  
6 (see Supplementary Material). The base run plume dispersion parameterisation used in this  
7 study is identical to that of Roberts et al., (2009), based on Pasquill-Gifford case D, with a  
8 SO<sub>2</sub> gas flux of 10 kg/s at a wind-speed of 10 m/s. The influence of variations in wind-speed  
9 (3-15 m/s), volcanic emission flux (10-20 kg/s SO<sub>2</sub>) and dispersion rates (Pasquill-Gifford  
10 case B,C,D) on downwind BrO/SO<sub>2</sub> ratios are also shown, as well as simulations with much  
11 greater volcanic emission flux (5× or 10× the base run). Volcanic aerosol loading in the  
12 model is investigated as part of the study, and for the majority of simulations is set to be 10<sup>-11</sup>  
13 μm<sup>2</sup> molec.SO<sub>2</sub><sup>-1</sup>, a factor of 10 lower than that of Roberts et al. (2009), following the  
14 *PlumeChem* model set-up used in Kelly et al. (2013).

15 The reaction of Br with BrONO<sub>2</sub> to form Br<sub>2</sub> + NO<sub>3</sub> (Orlando and Tyndall, 1996) was added  
16 to *PlumeChem* model in this study. This reaction influences the overall rate of HBr  
17 conversion into reactive bromine as follows: as a sink for BrONO<sub>2</sub> it slows the conversion of  
18 HBr into reactive bromine as less BrONO<sub>2</sub> undergoes heterogeneous uptake (which converts  
19 HBr into Br<sub>2</sub> via HOBr). However, as a sink for Br it slows the conversion of reactive  
20 bromine back into HBr from the reaction Br + HCHO. Under a high volcanic aerosol loading  
21 the former dominates, whilst the latter is more important at lower aerosol loadings. It is noted  
22 that this reaction is neither included in the IUPAC Kinetics nor JPL Data evaluation  
23 databases, thus is not necessarily included 'as standard' in all atmospheric models of reactive  
24 halogen chemistry.

25 BrNO<sub>2</sub> was suggested by von Glasow (2010) to be an important reservoir for Br in the near-  
26 downwind plume, based on assumed formation of BrNO<sub>2</sub> from volcanic NO<sub>x</sub> and Br radicals  
27 at a rate that exceeds BrNO<sub>2</sub> loss via photolysis. Formation of BrNO<sub>2</sub> was not included in  
28 previous *PlumeChem* model studies (Roberts et al., 2009, Kelly et al., 2013). Here, the fate of  
29 the products (BrNO<sub>2</sub> but also BrONO) from reaction of Br + NO<sub>2</sub> are investigated in more  
30 detail to evaluate the potential of BrNO<sub>2</sub> to influence the plume chemistry.

31

### 32 **3. Results**

### 3.1 Model SO<sub>2</sub> column abundance, and variability in simulated BrO/SO<sub>2</sub>

The formation of volcanic BrO is typically reported relative to SO<sub>2</sub>, which, given slow in-plume oxidation, acts as a plume tracer on the observation time-scales (typically minutes to hours). Therefore, prior to comparing *PlumeChem* model output to the observed BrO/SO<sub>2</sub>, a comparison is made between the simulated and reported SO<sub>2</sub> column abundances. Figure 1a shows slant SO<sub>2</sub> column abundance in Mt Etna's plume over 2004-2005, reported from DOAS (Differential Optical Absorption Spectroscopy) observations from Oppenheimer et al., (2006) and Bobrowski et al. (2007a). The data show a general decline with distance downwind, with the exception of two very near source measurements, which may have been underestimated in the very strong near-source plume, see discussion by Kern et al. (2012) and Bobrowski and Guiffrida (2012) for improved SO<sub>2</sub> evaluation. Also shown in Figure 1a is the model downwind plume SO<sub>2</sub> column abundance calculated for the plume in the vertical. The decline in modelled SO<sub>2</sub> column abundance with distance (or time) downwind is largely due to dispersion, given the slow rate of in-plume SO<sub>2</sub> oxidation. The rate of dispersion depends on plume depth, width, gas flux and wind-speed during each DOAS measurement, which are not fully constrained by available observations. Nevertheless, the broad agreement between model and observations indicates a suitable model parameterisation of plume-air mixing in the base run. This supports the use of further simulations to investigate the plume halogen chemistry using this plume-air mixing parameterisation scenario, for comparison to reported BrO/SO<sub>2</sub> observations.

Figure 1b shows formation of BrO (relative to plume tracer SO<sub>2</sub>) for a range of model simulations presented later in this study, all using this same plume-air mixing parameterisation, but where the other parameters (volcanic aerosol loading, total plume bromine, initialisation using thermodynamic model output) are varied. Clearly, these variables can have a strong influence on the downwind plume halogen chemistry. Also shown are BrO/SO<sub>2</sub> ratios reported by Oppenheimer et al. (2006) and the observed trend in (mean) BrO/SO<sub>2</sub> with distance downwind reported by Bobrowski et al., (2007). Several, but not all of the model simulations in Figure 1b conform to the BrO/SO<sub>2</sub> observations, . Indeed simulations whose initialisations assume no plume-air mixing at high-temperature typically underestimate downwind BrO/SO<sub>2</sub> (see section 3.3 for further discussion). The remaining model runs demonstrate broad agreement to the BrO/SO<sub>2</sub> measurements and provide an

1 explanation for the observed rise and subsequent plateau or decline in BrO/SO<sub>2</sub> with distance  
2 downwind reported by Bobrowski and Giuffrida (2012).

3 In order to provide further insight into the factors controlling volcano plume reactive halogen  
4 chemistry, we investigate here the influence of the abovementioned variables, and  
5 particularly uncertainties regarding the initialisation by HSC. To do so, suitable values for the  
6 volcanic bromine and aerosol loading are first identified, as outlined below.

7

### 8 **3.2. The effect of aerosol and bromine content on downwind BrO/SO<sub>2</sub>**

9 Highlighted in black in Figure 1b are four model runs that assume the ‘medium’ and ‘high’  
10 bromine (Br<sub>tot</sub>/SO<sub>2</sub>) emission scenarios (see Table 2), and two contrasting aerosol surface  
11 area loadings; namely ‘high’ aerosol estimated as  $\sim 10^{-10}$   $\mu\text{m}^2$  molec.SO<sub>2</sub><sup>-1</sup> following Roberts  
12 et al. (2009), and the ‘medium’ aerosol estimate, which is an order of magnitude lower,  $10^{-11}$   
13  $\mu\text{m}^2$  molec.SO<sub>2</sub><sup>-1</sup> as was used by Kelly et al. (2013). Both the volcanic aerosol loading and  
14 volcanic bromine content influence the downwind BrO/SO<sub>2</sub> evolution, as.

15 In general, a higher Br<sub>tot</sub>/SO<sub>2</sub> in the emission leads to greater BrO/SO<sub>2</sub> far downwind. This is  
16 in accordance with the proposed role of Br/S in the emission to explain order of magnitude  
17 variation in BrO/SO<sub>2</sub> ratios across Arc volcanoes (Roberts et al., 2009). A higher aerosol  
18 loading promotes the conversion of HBr into reactive forms, and promotes the occurrence of  
19 reactive bromine as BrO in the far downwind plume to its role in the heterogeneous reactive  
20 uptake of HOBr and BrONO<sub>2</sub>. Interestingly, whilst the volcanic aerosol and bromine content  
21 have a strong impact on the plateau in BrO/SO<sub>2</sub> far downwind (both in terms of value and  
22 when it is reached), Figure 1b indicates that aerosol and bromine content exert a much more  
23 limited impact on BrO/SO<sub>2</sub> in the very young plume during the first ~8 mins (~5 km) of  
24 plume evolution, at least for the plume dispersion conditions simulated. For example, at 36  
25 km downwind, the two contrasting aerosol loadings cause the model BrO/SO<sub>2</sub> to vary from  
26  $4.2 \cdot 10^{-4}$  to  $1.4 \cdot 10^{-3}$  (‘high’ bromine scenario) and from  $2 \cdot 10^{-4}$  to  $4 \cdot 10^{-4}$  (‘medium’ bromine  
27 scenario), whereas at 6 km downwind all of these model runs predict BrO/SO<sub>2</sub> between  
28  $2.5 \cdot 10^{-4}$  and  $4 \cdot 10^{-4}$ . This near-downwind similarity in BrO/SO<sub>2</sub> (despite varying Br<sub>tot</sub>/SO<sub>2</sub> as  
29 well as aerosol loading) is related to the role of oxidants in forming BrO, and differences in the  
30 proportion of HBr converted to reactive bromine. This predicted near-downwind  
31 independence of BrO/SO<sub>2</sub> on aerosol loading is consistent with the observations of

1 Bobrowski and Giuffrida (2012) at 6 km downwind that showed BrO/SO<sub>2</sub> was independent  
2 of relative humidity (a key control on sulphate aerosol volume hence surface area). A model  
3 explanation (see Section 3.4 for further discussion) is that near -downwind BrO/SO<sub>2</sub> ratios  
4 are primarily controlled by Br to BrO partitioning– itself a function of in-plume ozone mixing  
5 ratio - in this region where the plume is still relatively concentrated. See section 3.4 for  
6 details of the plume reactive bromine speciation and section 3.6 for further discussion on the  
7 plume impacts on atmospheric ozone.

8 Notably, the simulation with both ‘high’ bromine and the larger aerosol estimate predicts  
9 BrO/SO<sub>2</sub> that exceeds reported observations far downwind, and does not reproduce the  
10 plateau in BrO/SO<sub>2</sub> beyond ~ 5 km downwind of Etna summit recently reported by  
11 Bobrowski and Giuffrida (2012). We acknowledge the Etna bromine emission may vary with  
12 time therefore use both medium and high bromine emission scenarios alongside a low Br  
13 scenario in the further model simulations of this study. However, for the high bromine  
14 scenario, only the simulation with ‘medium’ aerosol surface area loading appears consistent  
15 with the BrO/SO<sub>2</sub> observations by Bobrowski and Giuffrida (2012). The ‘medium’ aerosol  
16 surface area loading is considered as likely being more representative and this estimate, ~10<sup>11</sup>  
17 μm<sup>2</sup> molec.SO<sub>2</sub><sup>-1</sup>, is used in all further model simulations of this study. Further discussion  
18 on estimates of the aerosol surface area loading is provided in Supplementary Material.

19

### 20 **3.3. The high-temperature near-vent plume - a source of model uncertainty**

21 An important model parameter in the *PlumeChem* model initialisation is the use of output  
22 from thermodynamic model HSC to represent the composition of the high-temperature near-  
23 vent plume.. Figure 2 compares the key species in the HSC output (Table 1) for the near-vent  
24 plume of Etna (‘medium’ Br scenario), using the standard HSC methodology, in which (a) H<sub>2</sub>  
25 and H<sub>2</sub>S re-equilibrate, and (b) the modified method (Martin et al., 2009) whereby H<sub>2</sub>S and  
26 H<sub>2</sub> do not re-equilibrate. NO, OH, Cl and Br and Cl<sub>2</sub> gas mixing ratios are shown for V<sub>A</sub>:V<sub>M</sub>  
27 ranging from 0:100 to 15:85, where V<sub>A</sub>:V<sub>M</sub> is the ratio of air to magmatic gases in the near-  
28 vent plume (plotted as a fraction in Figure 2), with the HSC temperature varied according to  
29 the mixture of magmatic (1050 °C) and ambient (20 °C) temperatures.

30 Of note is a step increase in radical mixing ratios in Figure 2a (in which H<sub>2</sub> and H<sub>2</sub>S re-  
31 equilibrate). This is the so-called compositional discontinuity, C.D., (Gerlach, 2004), which

1 occurs at around  $V_A:V_M \sim 0.02$  for Etna's magmatic composition. At the C.D., the reduced  
2 magmatic gases ( $H_2S$ ,  $H_2$ ,  $CO$ , etc) are essentially fully oxidised ( $SO_2$ ,  $H_2O$ ,  $CO_2$ ), thus  
3 addition of further oxidant (increasing  $V_A/V_M$ ) yields increases in the mixing ratios of the  
4 radicals (Br, Cl, NO, OH). As  $V_A:V_M$  increases further, the greater proportion of air relative  
5 to magmatic gases yields a lower HSC temperature, leading to slight declines or a plateau in  
6 the mixing ratios of NO and OH, and altering the balance between  $Cl_2$  and Cl radicals (Br<sub>2</sub>  
7 remains low over the whole  $V_A:V_M$  range). Formation of Br with increasing  $V_A:V_M$  also leads  
8 to a corresponding decrease in its 'parent' or 'source' species HBr (note other 'parent'  
9 species e.g. HCl,  $H_2O$  are in excess relative to  $Cl_x$  and OH). However, in the revised HSC  
10 methodology (in which  $H_2$  and  $H_2S$  do not re-equilibrate) the C.D. has shifted to low  $V_A:V_M$ ,  
11 as first shown by Martin et al. (2009). Indeed, it may no longer be relevant to talk of a C.D. at  
12 all, as an increase in radicals occurs immediately as  $V_A:V_M$  is increased; this is because the  
13 composition of the mixture is no longer buffered by magmatic  $H_2/H_2O$  and  $H_2S/SO_2$  ratios.

14 The fact that certain species need to be 'protected' from re-equilibration within presents a  
15 major limitation to the use of thermodynamic models to represent near-vent plume, as neither  
16 the choice of  $V_A:V_M$ , nor the protection of certain species (but not others) are fully justified  
17 on a physical basis. It is likely that some processes may be kinetics limited thus poorly  
18 described by thermodynamic models. Studies suggest this is indeed the case for formation of  
19  $NO_x$  from background  $N_2$  entrained into the plume (Martin et al. 2012), due to the high bond-  
20 strength for  $N_2$  (945 kJ/mol). Nevertheless, some evidence for the high-temperature  
21 formation of radicals in the near-vent plume, for example in the presence of crater-rim  
22 sulphate at  $SO_4^{2-}:SO_2 \sim 1:100$  (e.g. Mather et al., 2003, Martin et al., 2008), from which near-  
23 vent  $SO_3$  production might be inferred. Further, a volcanic source of  $HO_x$  is suggested by  
24 plume  $H_2O_2$  observations of Carn et al. (2011), a source of  $HO_x$  and  $NO_x$  is suggested by  
25 observations of  $HO_2NO_2$  at Erebus (Oppenheimer et al. 2010), and elevated NO and  $NO_2$  in  
26 plumes of Masaya (Mather et al. 2004) and Mt St Helens (see Martin et al., 2012 and  
27 references therein). Given abovementioned kinetic limitations to near-vent  $NO_x$  production  
28 from entrained background air, these results imply the need for alternative explanations for  
29  $NO_x$  at volcanoes where it has been reported, and raise the possibility that volcano  $NO_x$   
30 emissions at other volcanoes (e.g. Etna) might be lower than predicted by HSC.

31 A representation of high-temperature radical formation in the near-vent plume is, however,  
32 necessary for the initialisation of atmospheric chemistry models of downwind BrO chemistry.

1 The HSC model output is thus used for this purpose, despite above-mentioned limitations.  
2 Figure 3 shows 1 hr *PlumeChem* model simulations for the three bromine emission scenarios  
3 (low, medium, high), initialised using HSC operated at a range of  $V_A:V_M$  varying from 0:100,  
4 2:98, 5:95, 10:90 to 15:85, compared to reported BrO/SO<sub>2</sub> ratios from Oppenheimer et al.  
5 (2006) and Bobrowski et al. (2007). Simulations initialised with  $V_A:V_M$  of 0:100 (i.e. with no  
6 air mixed into the near-vent plume) under-predict BrO/SO<sub>2</sub> ratios compared to the  
7 observations, as has been shown previously (e.g. Bobrowski et al., 2007, Roberts et al., 2009,  
8 von Glasow, 2010) using atmospheric chemistry models. This is due to the low radical  
9 content at  $V_A:V_M = 0:100$  as shown in Figure 2). Previous studies therefore chose HSC  
10 initialisations using  $V_A:V_M > 0:100$ , e.g. Roberts et al. (2009) suggested  $V_A:V_M = 10:90$ , Von  
11 Glasow (2010) suggested  $V_A:V_M = 15:85$ . Given the revised location of the compositional  
12 discontinuity outlined above in Figure 2, even lower  $V_A:V_M$  e.g.  $V_A:V_M = 2:98$  or  $V_A:V_M =$   
13  $5:95$  (shown in red) can become suitable. Further progress will require more sophisticated  
14 models to be developed e.g. to include full kinetic representations of chemical and mixing  
15 processes.

16 Nevertheless, an interesting feature of Figure 3 is that whilst choice of HSC initialisation  
17 affects the 1 hr downwind plume BrO/SO<sub>2</sub> strongly, the model runs show a degree of  
18 convergence towards the end of the model run (particularly for low/medium Br cases).  
19 Understanding the < 1 hr plume chemistry is, however, important for interpretation of flank  
20 volcano BrO/SO<sub>2</sub> observations, and is investigated further with simulations initialised using  
21 HSC with  $V_A:V_M = 5:95$ .

22

### 23 **3.4. Speciation of reactive bromine in Etna plume and implications for** 24 **observations of volcanic BrO**

25 The evolution of reactive bromine speciation is also illustrated in Figure 3 for the three  
26 bromine emission scenarios, with simulations initialised using HSC at  $V_A:V_M = 5:95$ . A  
27 number of interesting features are identified:

- 28 • BrO/Br<sub>tot</sub> rises rapidly in the first few minutes, but then stabilises or declines further  
29 downwind.
- 30 • HBr is fully converted to reactive bromine in the ‘medium’ and ‘low’ bromine  
31 simulations but only partially converted in the ‘high’ bromine simulations.



- 1 • BrO is formed in the plume at up to 40-50 % ('medium' and 'low' Br emission  
2 scenario') or 10-20 % (high Br emission scenario) of total bromine. This difference is  
3 related to the extent of HBr conversion, as BrO reaches a similar maximum fraction  
4 (~50%) of reactive bromine in the three simulations
- 5 • An increase in plume BrCl occurs when HBr becomes depleted, which is due to the  
6 aqueous-phase equilibria producing substantial BrCl in place of Br<sub>2</sub>.
- 7 • HOBr and BrONO<sub>2</sub> are present in all simulations, and represent an increasing  
8 proportion of reactive bromine as the plume disperses downwind, whilst the  
9 proportion of BrO declines.

10 The observed and modelled trend in BrO/SO<sub>2</sub> shown in Figure 1 and 3 is thus explained as  
11 follows: HBr is converted into reactive forms by autocatalytic bromine chemistry cycles  
12 involving volcanic aerosol, entrained atmospheric oxidants and sunlight. The HBr conversion  
13 is accelerated by radical species present in the high-temperature initialisation. The initial rise  
14 in BrO/SO<sub>2</sub> primarily reflects trends in reactive bromine speciation; entrainment of  
15 background air containing ozone into the plume, promotes greater partitioning to BrO via the  
16 reaction Br + O<sub>3</sub>. Plume-air mixing is thus an important control on BrO/SO<sub>2</sub>, because the  
17 dilution of volcanic components and entrainment of air alter the balance between Br and BrO,  
18 e.g. by reducing the rate of BrO loss by the self-reaction BrO + BrO (to form 2Br or Br<sub>2</sub>), R7,  
19 relative to the formation of BrO by Br+O<sub>3</sub>, R6. The subsequent decline or plateau in BrO/SO<sub>2</sub>  
20 occurs due to net conversion of reactive bromine from BrO to HOBr and BrONO<sub>2</sub> in the  
21 downwind plume (R1, R2). These species are formed at an accelerated rate in the downwind  
22 plume as it disperses and entrains background air containing oxidants (HO<sub>2</sub>, NO<sub>2</sub>) which  
23 react with BrO. Further, the heterogeneous loss pathways for these species are slowed in the  
24 dispersed downwind plume where volcanic aerosol is diluted. The heterogeneous reactions of  
25 HOBr and BrONO<sub>2</sub> with aerosol present a more rapid loss pathway than photolysis in the  
26 aerosol-rich environment of a volcanic plume. As the plume disperses and dilutes further  
27 downwind, net accumulation of HOBr (and BrONO<sub>2</sub>) occurs whilst BrO declines (as a  
28 fraction of Br<sub>tot</sub>), although it is emphasized that plume chemistry cycling between these  
29 species is ongoing throughout the simulation and is very rapid.

30 This predicted reactive bromine evolution is somewhat similar to that of Roberts et al. (2009)  
31 but contrasts to the one hour simulations of von Glasow (2010) that did not predict the in-  
32 plume presence of HOBr and BrONO<sub>2</sub>. The higher proportion of total bromine as BrO in the

1 'medium' and 'low' Br emission scenarios (40-50 %) compared to the 'high' Br emission  
2 scenario (10-20 %) is related to the extent (complete and partial, respectively) of HBr  
3 conversion into reactive bromine species. This dependence of the HBr conversion on  
4  $\text{Br}_{\text{tot}}/\text{SO}_2$  in the emission may to some extent explain differences between the model studies  
5 of Roberts et al. (2009) and von Glasow (2010) that predicted complete and partial in-plume  
6 conversion of HBr into reactive bromine, respectively.

7 Predicted  $\text{BrO}/\text{SO}_2$  and  $\text{BrO}/\text{Br}_{\text{tot}}$  trends for the three Br emission scenarios (initialised with  
8  $V_{\text{A}}:V_{\text{M}} = 5:95$ ) are shown in Figure 4. The 'low' Br emission scenario simulation can be  
9 compared to observations by Oppenheimer et al. (2006) who reported (using DOAS)  
10  $\text{BrO}/\text{SO}_2$  ratios reached  $\sim 2 \times 10^{-4}$  within 3-4 minutes downwind of Etna summit, and used  
11 filter-packs to quantify the emitted  $\text{Br}_{\text{tot}}/\text{SO}_2$  to be  $4.8 \cdot 10^{-4}$ , i.e. implying a  $\text{BrO}/\text{Br}_{\text{tot}}$  of  $\sim 40$   
12 %. For the 'low' Br model run initialised at  $\text{Br}_{\text{tot}}/\text{SO}_2 = 4.8 \cdot 10^{-4}$ , which predicts complete  
13 conversion of HBr into reactive forms over 4 minutes,  $\text{BrO}/\text{SO}_2$  rises to  $10^{-4}$  within 4  
14 minutes, reaching a maximum of  $2.5 \cdot 10^{-4}$  at about 18 minutes downwind (i.e. earlier than the  
15 'medium' and 'high' bromine cases of this study) afterwhich  $\text{BrO}/\text{SO}_2$  declines, Figure 4a.  
16  $\text{BrO}/\text{Br}_{\text{tot}}$  reaches 25 % within 4 minutes, and 40 % by about 8 minutes (Figure 4b), thus  
17 converging towards the observations of Oppenheimer et al. (2006): the agreement is  
18 relatively good considering the predicted  $\text{BrO}/\text{Br}_{\text{tot}}$  can also be affected by other model  
19 parameters kept constant here e.g. in HSC initialisation, rate of plume-air mixing, aerosol  
20 loading, whilst observations of  $\text{BrO}/\text{Br}_{\text{tot}}$  are subject to measurement uncertainties e.g. in  
21 filterpack Br/S, DOAS measurement of  $\text{BrO}/\text{SO}_2$ .

22 The non-linearity of HBr conversion to BrO shown in Figure 4 yields the following  
23 implications for volcanology:  $\text{BrO}/\text{SO}_2$  ratios for these simulations (initialised at  $V_{\text{A}}:V_{\text{M}} =$   
24  $5:95$ ) reach maxima of  $3.6 \cdot 10^{-4}$  and  $4.6 \cdot 10^{-4}$  and  $2.5 \cdot 10^{-4}$  for the medium, high and low Br  
25 scenarios respectively in the downwind plume. Thus, whilst the modelled bromine emission  
26 has varied by a factor of three between the 'medium' and 'high' bromine scenarios, the  
27 simulated  $\text{BrO}/\text{SO}_2$  ratio has varied by less than 30 %. This result for small-scale bromine  
28 variations contrasts to the earlier *PlumeChem* simulations (Roberts et al., 2009) that  
29 suggested order of magnitude differences in  $\text{BrO}/\text{SO}_2$  between Souffrière Hills volcano  
30 ( $\text{BrO}/\text{SO}_2 \sim 10^{-3}$ ) and other Arc volcanoes like Etna ( $\text{BrO}/\text{SO}_2 \sim 10^{-4}$ ) could be attributed to  
31 order of magnitude differences in the ratio of total bromine to  $\text{SO}_2$  in their emissions.  
32 However, the non-linear relationship between BrO and emitted HBr, as identified in Figure 4

1 for small-scale bromine variations, presents a complexity to efforts to quantify volcanic  
2 bromine emissions using DOAS observations of plume BrO/SO<sub>2</sub> ratios within volcano  
3 monitoring programmes, and to modelling efforts to quantify impacts from volcanic halogen  
4 emissions to the troposphere. Nevertheless, DOAS observations (e.g. Bobrowski et al. 2003;  
5 2007b) do suggest a positive correlation between BrO/SO<sub>2</sub> and volcanic HBr emissions. For  
6 Soufrière Hills volcano, where high Br/S in the emission was proposed to lead to high plume  
7 BrO/SO<sub>2</sub>, further aspects to consider include the low altitude emission where ambient  
8 humidity and background aerosol might be high, potentially promoting both BrO chemistry  
9 and SO<sub>2</sub> oxidation rates.

10 Further understanding of the extent to which volcanic bromine is rapidly converted into  
11 reactive forms in the near-downwind plume is needed as part of efforts to evaluate global  
12 impacts from volcanic halogen degassing. Further studies of the wider model parameter space  
13 can contribute to this aim, although more observations are also needed to constrain model  
14 uncertainty. Overall, the model suggests HBr conversion into reactive bromine depends on a  
15 balance between the autocatalytic “bromine explosion” cycles in the near-downwind plume  
16 (accelerated by radicals produced in the high-temperature near-vent plume), and the  
17 conversion of reactive bromine back into HBr (e.g. via the reaction Br + HCHO).

18

### 19 **3.5 Low in-plume prevalence of BrNO<sub>2</sub>**

20 Formation of BrNO<sub>2</sub> from Br + NO<sub>2</sub> was excluded from the 1hr simulations presented in  
21 Figure 3 and 4. However, the plume chemistry modelling study of von Glasow (2010)  
22 predicted high in-plume prevalence of BrNO<sub>2</sub>, due to reaction of Br with NO<sub>2</sub>, given high Br  
23 and NO<sub>x</sub> mixing ratios are assumed in the (HSC) model initialisation. In the Etna simulations  
24 of von Glasow (2010) formation of BrNO<sub>2</sub> exceeds its photolytic loss rate in the young  
25 plume, leading to a significant partitioning (> 30 %) of plume bromine as BrNO<sub>2</sub>. To further  
26 evaluate this model difference, a similar two-reaction scheme for BrNO<sub>2</sub> was introduced into  
27 the *PlumeChem* model, with BrNO<sub>2</sub> the assumed (sole) product of the reaction Br + NO<sub>2</sub>.  
28 With this two-reaction scheme, model runs for the three bromine scenarios also show rapid  
29 formation of BrNO<sub>2</sub>, Figure 5 (acd). The in-plume BrNO<sub>2</sub> prevalence (< 30 % of plume  
30 bromine declining to just a few percent after 30 minutes), is still somewhat less than that of  
31 von Glasow (2010), and model differences remain in Br-speciation regarding presence of  
32 HOBr and BrONO<sub>2</sub>, potentially due to differences between the models’ aerosol loading or

1 dispersion schemes. Figure 5 (acd) highlights that the rapid formation of BrNO<sub>2</sub> in these  
2 model runs causes a slight delay to the formation of BrO downwind compared to the standard  
3 model runs of Figure 3.

4 However, we do not recommend use of the two-reaction BrNO<sub>2</sub> scheme, because the  
5 chemistry is in fact more complex. Firstly, the reaction Br + NO<sub>2</sub> primarily produces BrONO  
6 (~92%) rather than BrNO<sub>2</sub> (~8%), Bröske and Zabel (1998), Orlando and Burkholder (2000).  
7 Secondly, BrONO undergoes a more rapid thermal dissociation ( $\tau \sim 1$  s at room temperature),  
8 and photolytic loss ( $\tau \sim$  seconds) than BrNO<sub>2</sub>, Burkholder and Orlando (2000). BrONO and  
9 BrNO<sub>2</sub> also react with NO<sub>2</sub> (Bröske and Zabel, 1998). BrONO (and possibly also BrNO<sub>2</sub>)  
10 also react with Br radicals. The reactions are summarized in Table 3. *PlumeChem* simulations  
11 using a more detailed reaction scheme for BrNO<sub>2</sub>-BrONO-BrNO, incorporating the  
12 quantified reactions of Table 3, are illustrated in Figure 5 (bdf). With this revised BrNO<sub>2</sub>-  
13 BrONO-BrNO model scheme, these species account for only < 12 % of reactive bromine  
14 (with BrONO and BrNO at only < 1%). The impact of this scheme on Br-speciation is rather  
15 modest but some differences can be seen in comparison to the ‘standard’ simulations of  
16 Figure 3; for example a slightly faster rate of HBr conversion to reactive bromine. However,  
17 this more detailed reaction scheme is itself limited in that it does not include reaction of  
18 BrNO<sub>2</sub> with Br (rate constant unknown), and assumes the two possible BrONO photolysis  
19 pathways occur equally (as products are unknown). Further, the scheme does not include  
20 potential heterogeneous reactions relevant for BrNO<sub>2</sub>. Heterogeneous reactive uptake of N<sub>2</sub>O<sub>5</sub>  
21 might produce BrNO<sub>2</sub> or ClNO<sub>2</sub>, however, these products might react further within the  
22 aerosol to form Br<sub>2</sub> or BrCl (Frenzel et al. 1998). Proper investigation of such heterogeneous  
23 chemistry on volcanic aerosol would require detailed consideration of the underlying rate  
24 constants for all the aqueous-phase reactions (e.g. in a manner similar to that recently  
25 attempted for HOBr reactive uptake, Roberts et al., 2014). In addition to uncertainty in the  
26 model chemistry, the model findings are also subject to uncertainty in the HSC initialisation  
27 (which determines the volcanic Br and NO<sub>2</sub> radical source), see Section 3.3. Nevertheless, the  
28 more detailed reaction BrNO<sub>2</sub>-BrONO-BrNO scheme findings suggest the influence of  
29 BrNO<sub>2</sub> on the plume chemistry is much lower than that proposed by von Glasow (2010).  
30 Further simulations of this study therefore do not include BrNO<sub>2</sub>.

31

### 32 **3.6 Influence of plume-air mixing on BrO formation and ozone depletion**

1 Here we investigate the role of plume-air mixing on the (low-temperature) halogen chemistry  
2 evolution of the downwind plume. A first study investigates small variations as might be  
3 expected on a day-to-day basis at Etna. A second study investigates how large variations in  
4 the volcanic emission flux (e.g. due to an eruption) influence the plume chemistry, albeit  
5 within the limitations of an idealised model scenario.

6

### 7 **3.6.1 Influence of plume dispersion parameters, volcanic emission flux and** 8 **wind-speed on BrO/SO<sub>2</sub>**

9 As already discussed in Section 3.4, BrO formation is initially promoted by the entrainment  
10 of background air (containing ozone, HO<sub>x</sub> and NO<sub>x</sub>), due to the balance between the reaction  
11 Br + O<sub>3</sub> (R6) and the self-reaction of BrO (R7), but as the plume becomes more diluted the  
12 entrainment of air acts to reduce BrO/SO<sub>2</sub> due to the reaction of BrO with HO<sub>2</sub> and NO<sub>2</sub> (R1,  
13 R2). Thus, the proportion of background air that has been entrained into the plume acts as a  
14 key control on BrO/SO<sub>2</sub>. In the single-box Gaussian plume dispersion model used here, the  
15 extent of mixing of the background air into the plume is controlled by the Pasquill-Gifford  
16 dispersion parameters as a function of distance downwind, and whose choice depends on  
17 atmospheric turbulence (a function of wind-speed and atmospheric stability). Further, for a  
18 given dispersion parameterisation, the extent of mixing depends inversely on the volcanic  
19 emission flux, and also depends on wind-speed (through dilution along the plume). Here the  
20 effects of these three variables are illustrated for a range of plausible volcanic and  
21 meteorological conditions at Etna.

22 For the base run simulations (Figure 3-4), a Pasquill-Gifford (PG) dispersion case D was  
23 used, that is for a relatively neutral atmosphere, with a wind-speed of 10 m/s and volcanic gas  
24 flux of 10 kg/s SO<sub>2</sub> (with the emission of all other volcanic gas and aerosol components  
25 scaled accordingly). This SO<sub>2</sub> flux estimate is close to the ~13 kg/s reported by McGonigle et  
26 al. (2005) for 30 July 2004. The model 10 kg/s SO<sub>2</sub> flux is, however, a somewhat low  
27 representation for Mt Etna during 2004-5 in general. Aiuppa et al. (2005) report gas flux data  
28 that show summer-time variations between 800-2000, equivalent to 9-23 kg/s SO<sub>2</sub>, with even  
29 greater SO<sub>2</sub> flux during eruption periods. Burton et al. (2005) report 7-day average SO<sub>2</sub> fluxes  
30 of 1000-2500 t/d (12-25 kg/s). To illustrate the influence of variation gas flux and plume  
31 dispersion, simulations were also performed at 20 kg/s SO<sub>2</sub> flux, and for a range of dispersion  
32 and wind-speed cases. Cases C and B are introduced for more unstable atmospheric

1 conditions involving enhanced plume-air mixing, which occur more readily at lower wind-  
2 speed ( $< 6$  m/s), see Supplementary Material.

3 Simulations performed at wind-speeds of 10 m/s (case D and C), 15 m/s (case D and C), 5  
4 m/s (case D and C), and 3 m/s (case C and B) are shown in Figure 6 (a ‘medium’ bromine  
5 scenario is assumed for all these simulations, with  $V_A:V_M = 5:95$  in the initialisation). The  
6 model runs illustrate how plume-air mixing may cause variation in the downwind BrO/SO<sub>2</sub>.  
7 The variation is of a similar magnitude to that identified in the model runs with the three  
8 bromine scenarios, Figure 4 (which themselves encompass only a portion of the reported  
9 variability in Br/S in the emission, see Aiuppa et al., 2005). The model runs suggest that a  
10 combination of variations in plume-air mixing and bromine emission could provide – at least  
11 theoretically – a variability in BrO/SO<sub>2</sub> similar to the observed variability in BrO/SO<sub>2</sub> ( $5 \cdot 10^{-5}$   
12 -  $3.9 \cdot 10^{-4}$ ) reported by Bobrowski and Guiffrida (2012) at 6 km downwind. Variability in the  
13 volcanic aerosol emission could potentially add further to this.

14 Plume dispersion causes a transition between the two chemical regimes outlined above and  
15 an intermediate maximum in BrO/SO<sub>2</sub>. The magnitude and location of the downwind  
16 maximum in BrO/SO<sub>2</sub> depends on the extent of plume-air mixing, as determined by the gas  
17 flux, rate of dispersion and wind-speed, as well as on the volcanic aerosol loading and  
18 bromine content, and the HSC initialisation. Variations in background atmospheric  
19 composition (e.g. ozone, HO<sub>x</sub>, NO<sub>x</sub>, aerosol) could further modify the results. Finally, if  
20 applying these results to volcanoes elsewhere, the summit altitude is also a relevant  
21 consideration, as the greater atmospheric density at lower altitude will yield a higher in-  
22 plume ratio of background oxidants to bromine, for a given volcanic SO<sub>2</sub> flux.

23 Nevertheless, large increases in the volcanic emission flux tend to maintain for longer the  
24 more ‘concentrated’ regime where BrO/SO<sub>2</sub> is limited by the balance between R6 and R7, as  
25 discussed further below.

26

### 27 **3.6.2 Effect of a large increase in volcanic flux on BrO/SO<sub>2</sub>**

28 The sensitivity study is continued to for high emission scenarios by keeping the plume  
29 dispersion case and bromine emission scenario constant (case D, ‘medium’ Br<sub>tot</sub>/SO<sub>2</sub>), but  
30 increasing the volcanic gas and aerosol emission (by a factor of  $\times 5$  and  $\times 10$  of the base run  
31 10 kg/s SO<sub>2</sub> flux). Such an increased volcanic emission maintains higher concentrations of

1 volcanic gases thus reduces the extent of plume-air mixing, hence entrainment of background  
2 oxidants into the plume. We caution that in a real volcanic environment, such a large change  
3 in degassing rate may also be accompanied by a change in composition of the volcanic  
4 emission (including halogen content or aerosol loading) or act to alter the plume dimensions  
5 somewhat (e.g. by the dynamics of explosive eruptions). The model results here focus solely  
6 on the effect of (substantially) enhanced gas flux with all other variables held constant.

7 Simulations of three hours duration (equivalent to 108 km downwind plume propagation  
8 assuming 10 m/s windspeed) with volcanic emission flux increased from the base run to  $\times 5$   
9 and  $\times 10$  are shown in Figure 7, for both the ‘medium’ and ‘high’ bromine emission scenarios  
10 (initialised with HSC using  $V_A:V_M = 5:95$ ). The enhanced volcanic emission flux linearly  
11 enhances in-plume  $\text{SO}_2$  abundance, as expected, but exerts a non-linear effect on the plume  
12 chemistry and impacts.

13 In particular, the greater volcanic emission (lower plume-air mixing) leads to a slower rise,  
14 and a later onset and slower decline in  $\text{BrO}/\text{SO}_2$ . At distances far downwind ( $> 2$  hr for the  
15 specific simulation conditions), high  $\text{BrO}/\text{SO}_2$  is sustained for longer in plumes with high gas  
16 flux. Conversely, in the near downwind (several 10’s of mins), plumes with lowest gas flux  
17 exhibit the fastest initial rise and highest  $\text{BrO}/\text{SO}_2$  ratios. As described above, these model  
18 findings are readily explained by the model chemistry that partitions reactive bromine  
19 between  $\text{Br}$  and  $\text{BrO}$  (during the initial rise), and  $\text{BrO}$ , and  $\text{HOBr}$ ,  $\text{BrONO}_2$  (during the  
20 subsequent decline) as the plume disperses. The onset and magnitude of the decline is  
21 greatest for low flux plumes that are more dilute and where a higher proportion of  
22 background air has been mixed into the plume. Conversely, high flux thus more concentrated  
23 plumes have a slower initial increase in  $\text{BrO}/\text{SO}_2$ , with a delayed maximum. In the relatively  
24 near-downwind plume (0-30 minutes), the model predicts lower  $\text{BrO}/\text{SO}_2$  at greater volcanic  
25 gas fluxes, as shown by the arrows in Figure 6. Implications for the interpretation of volcano  
26 plume observations are discussed in Section 3.7.

27

### 28 **3.6.3 Atmospheric impacts of volcanic reactive halogen chemistry**

29  $\text{BrO}$  chemistry causes ozone,  $\text{HO}_x$  and  $\text{NO}_x$  to become depleted in the downwind plume,  
30 Figure 8. For  $\text{HO}_x$  and  $\text{NO}_x$  the near-downwind plume abundances are initially elevated as  
31 the HSC initialisations used assumed a volcanic source of these species (Figure 2), but

1 become depleted within a few to 10's minutes downwind. The maximum depletion reaches is  
2 near 100 % and > 70 % depletion relative to background values of around 30 pptv and 0.17  
3 ppbv for HO<sub>x</sub> and NO<sub>x</sub> respectively. HO<sub>x</sub> is converted into H<sub>2</sub>O<sub>(l)</sub> via HOBr chemistry (R1,  
4 R3). HO<sub>x</sub> abundances are also reduced by the gas-phase reaction of OH with SO<sub>2</sub>, and by  
5 ozone depletion in the plume (see below). The volcanic NO<sub>x</sub> source is converted into HNO<sub>3</sub>  
6 by BrONO<sub>2</sub> chemistry (R2, R4), causing a rapid increase in-plume HNO<sub>3</sub>, particularly in the  
7 concentrated near-downwind plume, where HNO<sub>3</sub> reaches up to 60 nmol/mol (exceeding the  
8 background NO<sub>y</sub> of ~6 nmol/mol). This mechanism was proposed by Roberts et al. (2009) as  
9 an explanation for observations of high HNO<sub>3</sub> in volcanic plumes. See collated observations  
10 by Martin et al. (2012) reporting plume HNO<sub>3</sub>/SO<sub>2</sub> that can reach up to 10<sup>-1</sup>. For Etna in  
11 particular, reported crater-rim HNO<sub>3</sub>/SO<sub>2</sub> ratios are somewhat inconsistent and show large  
12 variability (-2.3·10<sup>-4</sup>, 7.8·10<sup>-6</sup>, 4.2·10<sup>-3</sup>), which in itself might be indicative of a role of plume  
13 chemistry processing. Recently Voigt et al. (2014) also observed elevated HNO<sub>3</sub> in the  
14 downwind Etna plume, with HNO<sub>3</sub> as the dominant form of NO<sub>y</sub>. Importantly, elevated  
15 'volcanic' HNO<sub>3</sub> produced by the BrONO<sub>2</sub> mechanism can originate from both NO<sub>x</sub> of  
16 volcanic origin, and from NO<sub>x</sub> from background air entrained into the plume. As  
17 consequence, the in-plume NO<sub>x</sub> declines from initially elevated abundance (due to the  
18 assumed high temperature volcanic NO<sub>x</sub> source) to become depleted relative to the  
19 background abundance downwind. Finally, it is noted that simple acidification of nitrate  
20 aerosol from background air entrained into the plume could also lead to gas partitioning  
21 therefore enhance the 'volcanic' HNO<sub>3(g)</sub> signature. Such acid-displacement of HNO<sub>3(g)</sub> by  
22 H<sub>2</sub>SO<sub>4(aq)</sub> has been observed by Satsumabayashi et al. (2004). The observations of volcanic  
23 HNO<sub>3</sub> collated by Martin et al. (2012) and Voigt et al. (2014) thus require consideration in  
24 the context of these two mechanisms.

25

26 Ozone is also depleted in the plume and reaches a maximum depletion (up to 100%) around  
27 10 minutes downwind, coincident with the highest in-situ BrO abundances that reach ~ 1  
28 nmol/mol (Figure 7). For the base run, the maximum plume ozone depletion is 30 or 45  
29 nmol/mol for the medium and high bromine emission scenarios respectively. Greater in-  
30 plume ozone loss occurs at higher emissions flux (lower relative plume-air mixing), however  
31 for these runs the maximum ozone loss is constrained by the fact it cannot exceed ~60  
32 nmol/mol (the background ozone mixing ratio). Thereafter ozone begins to recover as the



1 plume disperses (Figure 8), entraining background air, and BrO declines (Figure 7), albeit at  
 2 a slower rate than the SO<sub>2</sub> plume tracer. Ozone recovery is greater for the base run than the  
 3 higher volcanic flux cases due to both physical and chemical consequences of enhanced  
 4 plume-air mixing. Thus presence of a detectable ozone depletion signature at distances far  
 5 downwind depends on the emission flux and plume-dispersion. Further, the single box  
 6 simulations presented here that predict the downwind trend do not simulate the ozone  
 7 distribution across the plume cross-section. Ozone loss is typically greater in the plume centre  
 8 than near the edges, see for example the spatially resolved model simulations for Redoubt  
 9 plume that assumes similar Gaussian plume dispersion (Kelly et al. 2013). The single-box  
 10 simulations should be interpreted in this context, e.g. a predicted loss of 45 nmol/mol implies  
 11 greater loss at the plume centre (likely close to 60 nmol/mol or 100 %) declining to near-  
 12 ambient ozone at the plume edges. For example spatially resolved model simulations for  
 13 Redoubt plume predicted greater loss in the plume centre than the edges (Kelly et al. 2013).  
 14 The ozone mixing ratio starts to increase when the entrainment of ambient air containing O<sub>3</sub>  
 15 is faster than the local O<sub>3</sub> destruction. Nevertheless, ongoing occurrence of ozone depleting  
 16 BrO chemistry is demonstrated by the continuing negative trend in the cumulative ozone loss:  
 17 the ozone difference (plume-background) integrated across the plume cross-sectional area  
 18 declines along the 3 hr simulations to reach ~1, 4, and 7 g/cm<sup>-1</sup> for the three flux scenarios  
 19 (SO<sub>2</sub> flux = 10, 50, 100 kg/s) respectively with greater ozone loss for the high Br compared to  
 20 the medium Br scenario, as expected. These Lagrangian simulations of plume ‘puff’ ozone  
 21 evolution over 3 hr can also be viewed in a Eulerian context: the 3 hr impact of continuous  
 22 volcano emissions is calculated by integrating the cross-sectional impact (g/cm<sup>-1</sup>) over the  
 23 distance downwind. This yields ozone losses of 35·10<sup>3</sup> (38·10<sup>3</sup>), 26·10<sup>3</sup> (23·10<sup>3</sup>), and 6·10<sup>3</sup>  
 24 (4·10<sup>3</sup>) kg for the ×10 flux, ×5 flux and base run (10 kg/s SO<sub>2</sub> flux) scenarios respectively the  
 25 assuming the medium Br scenario (numbers in brackets refer to high Br scenario). Whilst  
 26 there is some linearity in ozone loss per Br emitted (e.g. in comparing the base run to ×5 flux  
 27 cases), the constraint that ozone loss cannot exceed 100% of the background abundance  
 28 introduces some non-linearity for the ×10 flux case, thereby reducing its overall ozone loss.  
 29 Note that the plume cross-sectional area after 3 hrs is  $\pi \cdot \sqrt{2} \cdot \sigma_h \cdot \sqrt{2} \cdot \sigma_z = 2 \cdot \pi \cdot 4470 \cdot 485 = 1.4 \cdot 10^7$   
 30 m<sup>2</sup>. The volcanic plume cone thus resides within a cylinder of volume  $1.4 \cdot 10^7 \cdot 108 \cdot 10^3$   
 31 =  $1.5 \cdot 10^{12}$  m<sup>3</sup>, containing approx.  $110 \cdot 10^3$  kg ozone.

32 Figure 8 indicates that the plume atmospheric impacts extend beyond the one to three hour  
 33 simulations presented in this study. Simulations over the lifetime of volcanic plumes under

1 different volcanological and meteorological conditions are therefore required to quantify the  
2 global tropospheric impact from volcanic halogen emissions.

3

### 4 **3.7 Implications for modelling and observations of volcanic BrO**

5 The parameter space governing volcanic plume reactive halogen chemistry is vast, and is not  
6 fully constrained by available observations. Of particular importance in controlling the  
7 reactive bromine formation and downwind plume bromine speciation are:  $\text{Br}_{\text{tot}}/\text{SO}_2$  in the  
8 emission, the volcanic aerosol loading, and the extent of background air mixing into the  
9 plume (itself a function of the plume dispersion parameterisation, volcanic emission flux and  
10 wind-speed). These factors exert non-linear influences on the conversion of emitted HBr into  
11 plume reactive bromine, and its speciation through interconversion of BrO, Br, Br<sub>2</sub>, BrCl,  
12 HOBr, BrONO<sub>2</sub>.

13 The onset of the autocatalytic reactive bromine formation is also accelerated in the model by  
14 radicals in the high-temperature model initialisation (Br, Cl, NO<sub>x</sub>, HO<sub>x</sub>). A major area of  
15 uncertainty is, however, the representation of this high-temperature near-vent plume  
16 environment using thermodynamic models such as HSC. Development of high-temperature  
17 kinetic models of the near-vent plume is encouraged for progress in this area.

18 Further uncertainty to the downwind plume chemistry is contributed by uncertainty in the  
19 volcanic bromine emission, and in aerosol surface area, that sustains halogen cycling  
20 downwind. Crater-rim filter-pack measurements (e.g. Aiuppa et al., 2005) provide estimates  
21 of volcanic Br/S emissions for model initialisation (see Table 2) but also highlight temporal  
22 variability in this parameter. The volcanic aerosol emission is poorly constrained by  
23 observations at Etna, and from volcanoes globally. A surface area loading of  $\sim 10^{-11} \mu\text{m}^2$   
24 molec SO<sub>2</sub><sup>-1</sup>, i.e. an order of magnitude lower than that used by Roberts et al. (2009) yields  
25 simulated (0-20 km) downwind BrO/SO<sub>2</sub> more consistent with that observed in the Etna  
26 plume. Volcanic aerosol has a small influence on BrO/SO<sub>2</sub> ratio near source, but is an  
27 important control in the more dispersed plume downwind. Uncertainties in the volcanic  
28 aerosol emission magnitude, and its size distribution (which for sulfate varies as a function  
29 temperature and humidity) thus contribute to uncertainties in models of the plume halogen  
30 chemistry. Plume aerosol may be augmented by in-plume oxidation of volcanic SO<sub>2</sub> to  
31 H<sub>2</sub>SO<sub>4</sub>, and the entrainment and acidification of background aerosol may also promote

1 halogen cycling. Future model evaluation of volcanic reactive halogen impacts in the wider  
2 troposphere will require development of regional and global models, with detailed treatment  
3 of aerosol processes as well as plume dispersion (shown to be a key control on the downwind  
4 chemistry). An improved quantification of the kinetics of HOBr reactive uptake on volcanic  
5 aerosol is also needed according to Roberts et al. (2014). Global models may need to include  
6 a representation of the sub-grid scale volcanic plume processes, particularly as this study  
7 highlighted how the proportion of emitted HBr converted into reactive forms is non-linearly  
8 dependent on the degassing scenario.

9

10 We emphasize the complex role of plume chemistry in the interpretation of volcano flank  
11 DOAS measurements of BrO/SO<sub>2</sub>. Bobrowski and Giuffrida (2012) recently reported  
12 variation in BrO/SO<sub>2</sub> ratios at Etna related to the onset of eruption activity, for example with  
13 increasing BrO/SO<sub>2</sub> shortly prior to an eruptive event, and lower BrO/SO<sub>2</sub> during the eruption  
14 event, according to DOAS measurements 6 km downwind from the summit. These  
15 observations have been interpreted in the context of variable bromine and SO<sub>2</sub> emissions,  
16 related to subsurface magmatic processes. Lübcke et al. (2013) identified a decrease in  
17 BrO/SO<sub>2</sub> observed using a DOAS instrument prior to an eruption event at Nevado del Ruiz,  
18 Colombia (in a period whilst SO<sub>2</sub> emissions were increasing). However, we emphasize that a  
19 variation in plume BrO/SO<sub>2</sub> can also result from differences in the plume chemistry for  
20 varying volcanic emission flux magnitudes. Figure 6 shows that changes in volcanic gas flux  
21 (for a fixed plume dimension) can yield substantial changes in plume BrO/SO<sub>2</sub> ratio, even for  
22 a fixed Br<sub>tot</sub>:SO<sub>2</sub> ratio in the emission. In the near-downwind plume, a key control on BrO  
23 formation is the entrainment of oxidants. A substantial increase in volcanic emission flux  
24 leads to greater plume strength and reduced ratio of background oxidants to bromine in the  
25 model. Thus, on the <60 min timescale of volcano flank DOAS observations, a substantially  
26 enhanced rate of volcanic degassing generally leads to lower plume BrO/SO<sub>2</sub> ratios in more  
27 concentrated plumes. Potentially, the variations in BrO/SO<sub>2</sub> identified by Bobrowski and  
28 Giuffrida (2012), and Lübcke et al. (2013) may result from a combination of volcanological  
29 and plume chemistry factors. This example highlights the complexity surrounding  
30 interpretation of volcanic BrO and shows the role of plume chemistry modelling in the effort  
31 to use volcanic BrO observations to monitor and predict volcanic activity.

1 We also highlight that the plume chemical evolution causes a decline in BrO/SO<sub>2</sub> ratios in the  
2 dispersed plume further downwind through net conversion of BrO into reservoirs such as  
3 HOBr and BrONO<sub>2</sub>. This plume chemical evolution acts to reduce the BrO column  
4 abundance, contributing additional limitations to its possible detection in dispersed plumes,  
5 and is the model explanation for the plateau in BrO/SO<sub>2</sub> downwind of Etna reported by  
6 Bobrowski and Guiffrida (2012). Detection of volcanic BrO by satellite is primarily  
7 constrained to large volcanic emissions (Theys et al., 2009, Rix et al. 2012, Hörmann et al.,  
8 2013). Smaller volcanic emissions that generate high but localised BrO at lower altitudes are  
9 less readily detected particularly due to dilution effects across the satellite measurement pixel  
10 (Afe et al., 2004). The modelled plume chemical evolution adds to this limitation for satellite  
11 detection of BrO in dispersed volcanic plumes (even at higher resolution). Importantly,  
12 however, the model Br-speciation shows that a declining trend in BrO abundance as the  
13 volcanic plume disperses does not preclude the occurrence of continued in-plume reactive  
14 bromine chemistry as predicted by the model.

15

#### 16 **4. Conclusion**

17 We present a *PlumeChem* model study of the reactive halogen chemistry of Mt Etna volcano  
18 plume that reproduces the recently reported trends in BrO/SO<sub>2</sub>; namely a rapid increase in the  
19 near-downwind followed by stability or decline in the far-downwind. A new in-plume  
20 evolution of Br-speciation is predicted: BrO Br<sub>2</sub>, Br and HBr are the main plume species in  
21 the near downwind plume whilst BrO, HOBr (and BrONO<sub>2</sub>, BrCl) are present in significant  
22 quantities further downwind. An evaluation of the (quantifiable) chemistry surrounding  
23 BrNO<sub>2</sub> suggests a rather low prevalence in volcanic plumes, although uncertainties in model  
24 chemistry and initialisation are highlighted.

25 Emitted volcanic HBr is converted into reactive bromine by autocatalytic bromine chemistry  
26 cycles whose onset is accelerated by the model high-temperature initialisation. The initial rise  
27 in BrO/SO<sub>2</sub> is primarily due to entrainment of ozone through plume dispersion that promotes  
28 BrO formation from Br radicals. A subsequent decline or plateau in BrO/SO<sub>2</sub> occurs upon  
29 plume dispersion, which both dilutes the volcanic aerosol (slowing HOBr and BrONO<sub>2</sub>  
30 heterogeneous loss rates) and entrains HO<sub>2</sub> and NO<sub>2</sub> from the background atmosphere  
31 (promoting HOBr and BrONO<sub>2</sub> formation from BrO). This promotes net accumulation of  
32 reservoirs HOBr and BrONO<sub>2</sub> and a reduction in BrO in the dispersed downwind plume.

1 Thus the model can explain the reported BrO/SO<sub>2</sub> trend at Etna. We demonstrate the role of  
2 plume chemistry models to interpret volcanic BrO/SO<sub>2</sub> observations as well as quantify  
3 atmospheric impacts on HO<sub>x</sub>, NO<sub>x</sub>, HNO<sub>3</sub> and ozone. A number of volcanological and  
4 meteorological factors can influence plume BrO/SO<sub>2</sub> ratios, and we illustrate simulations  
5 with contrasting total bromine content and volcanic aerosol loading. The influence of plume-  
6 air mixing is shown by simulations with varying dispersion rate, as well as wind-speed and  
7 volcanic gas flux.

8 BrO contents reach up to 20% and ~50% of total bromine (over a timescale of a few 10's of  
9 minutes), for the high and medium/low bromine emission scenarios, respectively. The latter  
10 agrees well with observations that report BrO (at 3-5 min downwind) can reach up to 40% of  
11 the total bromine emission at Etna (Oppenheimer et al., 2006). Partial (up to ~50%) or  
12 complete (100%) conversion of HBr to reactive forms is predicted over the one hour  
13 simulations, depending on bromine content (high, medium or low, respectively) as well as  
14 other the plume conditions (e.g. aerosol, dispersion, HSC initialisation). Simulations using  
15 the two volcanic aerosol loadings significantly differ in the downwind plume chemistry but  
16 result in a similar initial rise in BrO/SO<sub>2</sub> near-downwind (up to 6 km), a finding that is in  
17 agreement with the reported low relative humidity dependence of BrO/SO<sub>2</sub> (Bobrowski and  
18 Giuffrida, 2012).

19 Simulations with a fixed dispersion rate but enhanced volcanic emission flux are presented.  
20 For higher emission fluxes, the stronger plume and reduced ratio of background  
21 oxidants:bromine causes a slower rise in BrO/SO<sub>2</sub> in the near downwind plume (< 40 min)  
22 and a slower and delayed onset of the decrease in BrO/SO<sub>2</sub> in the far downwind plume (> 2  
23 hr, for the volcanic conditions simulated). This simulated dependence of BrO/SO<sub>2</sub> on  
24 volcanic emission flux (albeit in an idealised model scenario) is particularly relevant towards  
25 the interpretation of changes in BrO/SO<sub>2</sub> during/prior to eruptive events (e.g. Bobrowski and  
26 Giuffrida, 2012, Lübcke et al., 2013).

27 Impacts of the plume halogen chemistry include downwind depletion of HO<sub>x</sub>, NO<sub>x</sub> and  
28 ozone, and formation of HNO<sub>3</sub>. Partial recovery of ozone is predicted, particularly for low  
29 gas flux emissions. However cumulative impacts on ozone are ongoing over the 3 h  
30 simulations.

31

1  
2  
3  
4  
5  
6  
7  
8  
9  
10  
11  
12  
13  
14  
15  
16  
17  
18  
19  
20  
21  
22  
23  
24  
25  
26  
27  
28  
29

## Acknowledgements

This study was financed by LABEX VOLTAIRE (VOLatils- Terre Atmosphère Interactions - Ressources et Environnement) ANR-10-LABX-100-01 (2011-20) and an NSINK career development allowance that enabled HSC software purchase. RSM acknowledges Christ's College, Cambridge for a research fellowship. Contributions of authors: TJR designed and performed the *PlumeChem* model experiments and HSC calculations and wrote the manuscript. RSM advised on HSC methodology and contributed to manuscript writing. LJ advised on scientific scope and contributed to manuscript writing.

## References

Afe O.T., Richter A., Sierk B., Wittrock F., and Burrows J.P.: BrO emission from volcanoes: A survey using GOME and SCIAMACHY measurements, *Geophysical Research Letters*, 31, L24113, doi:10.1029/2004GL020994, 2004.

Aiuppa A., Federico C., Franco A., Giudice G., Guierri S., Inguaggiato, Liuzzo M., McGonigle A.J.S., Valenza M.: Emission of bromine and iodine from Mount Etna volcano, *Geochemistry, Geophysics, Geosystems*, 6,8, Q08008, doi:10.1029/2005GC000965, 2005.

Aiuppa, A., Shinohara H., Tamburello G., Giudice G., Liuzzo M., Moretti R.: Hydrogen in the gas plume of an open-vent volcano, Mount Etna, Italy, *Journal of Geophysical Research*, 116, B10204, doi:10.1029/2011JB008461, 2011.

Bagnato E., Aiuppa A., Parello F., Calabrese S., D'Alessandro W., Mather T.A., McGonigle A.J.S., Pyle D.M., Wangberg I.: Degassing of gaseous (elemental and reactive) and particulate mercury from Mount Etna volcano (Southern Italy), *Atmospheric Environment*, 41,7377–7388, 2007.

1 Baker, A. K., Rauther- Schöch A., Schuck T. J., Brenninkmeijer C. A. M., van Velthoven P.  
2 F. J. Wisner A., Oram D. E., Investigation of chlorine radical chemistry in the  
3 Eyjafjallajökull volcanic plume using observed depletions in non-methane hydrocarbons,  
4 Geophysical Research Letters, 38, L13801, doi:10.1029/2011GL047571, 2011.  
5  
6 Bani P., Oppenheimer C., Tsanev V. I., Carn S. A., Cronin S. J., Crimp R., Calkins, J. A.,  
7 Charley D., Lardy M., and Roberts T.J.: Surge in sulphur and halogen degassing from  
8 Ambrym volcano, Vanuatu, B. Volcanol., 71, 10, 1159–1168, DOI 10.1007/s00445-009-  
9 0293-7, 2009.  
10  
11 Bobrowski, N., Honniger, G., Galle, B. and Platt, U.: Detection of bromine monoxide in a  
12 volcanic plume. Nature, 423, 273-276, doi:10.1038/nature01625, 2003.  
13  
14 Bobrowski, N., von Glasow, R., Aiuppa, A., Inguaggiato, S., Louban, I., Ibrahim, O. W.  
15 and Platt, U.: Reactive halogen chemistry in volcanic plumes, J. Geophys. Res., 112, D06311,  
16 doi:10.1029/2006JD007206, 2007a.  
17  
18 Bobrowski, N. and Platt, U.: SO<sub>2</sub>/BrO ratios studied in five volcanic plumes. J. Volcanol.  
19 Geoth. Res., 166, 3-4, 147-160, 10.1016/j.jvolgeores.2007.07.003, 2007b.  
20  
21 Bobrowski N. and G. Giuffrida: Bromine monoxide/sulphur dioxide ratios in relation to  
22 volcanological observations at Mt. Etna 2006–2009, Solid Earth, 3, 433–445, doi:10.5194/se-  
23 3-433-2012, 2012.  
24  
25 Boichu, M., Oppenheimer C., Roberts T. J., Tsanev V., Kyle P. R.: On bromine, nitrogen  
26 oxides and ozone depletion in the tropospheric plume of Erebus volcano (Antarctica), Atmos.  
27 Environ., 45, 23, 3856-3866, 2011.  
28

1 Bröske R. and Zabel F.: Kinetics of the Gas-Phase Reaction of BrNO<sub>2</sub> with NO, J. Phys.  
2 Chem. A 1998, 102, 8626-8631  
3

4 Burkholder J. B. and Orlando J. J., UV absorption cross-sections of cis-BrONO, Chemical  
5 Physics Letters, 317, 6, 603–608, 2000.  
6

7 Burton, M. R., Neri M., Andronico D., Branca S., Caltabiano T., Calvari S., Corsaro R. A.,  
8 Del Carlo P., Lanzafame G., Lodato L., Miraglia L., Salerno G., and Spampinato L.: Etna  
9 2004–2005: An archetype for geodynamically-controlled effusive eruptions, Geophys. Res.  
10 Lett., 32, L09303, doi:10.1029/2005GL022527, 2005.  
11

12 Carn S. A, Froyd K. D., Anderson B. E., Wennberg P., Crouse J., Spencer K., Dibb J. E.,  
13 Krotkov N. A., Browell E. V., Hair J. W., Diskin G., Sachse G., and Vay S. A., In situ  
14 measurements of tropospheric volcanic plumes in Ecuador and Colombia during TC, Journal  
15 of Geophysical Research, 116, D00J24, doi:10.1029/2010JD014718, 2011.  
16

17 Frenzel A., Scheer V., Sikorski R., George Ch., Behnke W., Zetzsch C.: Heterogeneous  
18 Interconversion Reactions of BrNO<sub>2</sub>, ClNO<sub>2</sub>, Br<sub>2</sub>, and Cl<sub>2</sub>, J. Phys. Chem. A, 102, 1329-  
19 1337, 1998.  
20

21 Gerlach, T.M.: Volcanic sources of tropospheric ozone-depleting trace gases, Geochemistry.  
22 Geophysics. Geosystems (G<sup>3</sup>) 5, Q09007, doi:10.1029/2004GC000747, 2004.  
23

24 Giggenbach, W.F.: Redox processes governing the chemistry of fumarolic gas discharges  
25 from White Island, New Zeland, Appl. Geochem., 2, 143-161, 1987.  
26

27 Grimley, A. J.; Houston, P. L. The photochemistry of nitrosyl halides: The X+NOX--  
28 >X<sub>2</sub>+NO(v) reaction (X=Cl, Br), J. Chem. Phys. 72, 1471, 1980.



1  
2  
3  
4  
5  
6  
7  
8  
9  
10  
11  
12  
13  
14  
15  
16  
17  
18  
19  
20  
21  
22  
23  
24  
25  
26  
27  
28  
29

Heue, K.-P., Brenninkmeijer, C.A.M., Baker, A. K., Rauthe-Schöch, A., Walter, D., Wagner, T., Hörmann, C., Sihler, H., Dix, B., Frieß, U., Platt, U., Martinsson, B. G., van Velthoven, P. F. J., Zahn, A. and Ebinghaus, R.: SO<sub>2</sub> and BrO observation in the plume of the Eyjafjallajökull volcano 2010: CARIBIC and GOME-2 retrievals, *Atmos. Chem. Phys.*, 11, 2973-2989, doi:10.5194/acp-11-2973-2011, 2011.

Hippler, H.; Luu, S. H.; Teitelbaum, H. and Troe, J.: Flash photolysis study of the NO-catalyzed recombination of bromine atoms, *Int. J. Chem. Kinet.* 10, 155. 1978.

Hobbs, P. V., Tuell, J. P., Hegg, D. A., Radke, L. F. and Eltgroth, M. W.: Particles and gases in the emissions from the 1980-1981 volcanic eruptions of Mt. St. Helens., *J. of Geophys. Res.*, 87, C13, 11062-11086, 1982.

Hörmann C., Siöler H., Bobrowski N., Beirle S., Penning de Vries M., Platt U., and Wagner T.: Systematic investigation of bromine monoxide in volcanic plumes from space by using the GOME-2 instrument, *Atmos. Chem. Phys.*, 13, 4749–4781, 2013.

Kelly P.J., Kern C., Roberts T.J., Lopez T., Werner C., and Aiuppa A.: Rapid chemical evolution of tropospheric volcanic emissions from Redoubt Volcano, Alaska, based on observations of ozone and halogen-containing gases, *Journal of Volcanology and Geothermal Research*, *Journal of Volcanology and Geothermal Research*, 259, 317–333, 2013.

Kern, C., Sihler, H., Vogel, L., Rivera, C., Herrera, M. and Platt, U.: Halogen oxide measurements at Masaya Volcano, Nicaragua using active long path differential optical absorption spectroscopy, *B. Volcanol.*, 71, 6, 659-670, 2009.

Kern, C., T. Deutschmann, C. Werner, A. J. Sutton, T. Elias, and P. J. Kelly (2012), Improving the accuracy of SO<sub>2</sub> column densities and emission rates obtained from upward-

1 looking UV-spectroscopic measurements of volcanic plumes by taking realistic radiative  
2 transfer into account, *J. Geophys. Res.*, 117, D20302, doi:10.1029/2012JD017936.

3

4 Louban I., Bobrowski N. , Rouwet D., Inguaggiato S., and Platt U.: Imaging DOAS for  
5 volcanological applications, *Bulletin of Volcanology*, 71, 753–765, 2009.

6

7 Lübcke P., Bobrowski, N., Arellano, S., Galle, B., Garzón, G., Vogel, L., Platt U., BrO/SO<sub>2</sub>  
8 molar ratios from scanning DOAS measurements in the NOVAC network, *Solid Earth*  
9 *Discuss.*, 5, 1845–1870, 2013.

10

11 Martin, R. S., Mather, T. A. and Pyle, D. M.: High-temperature mixtures of magmatic and  
12 atmospheric gases, *Geochemistry, Geophysics, Geosystems (G<sup>3</sup>)*, 7, Q04006,  
13 doi:10.1029/2005GC001186, 2006.

14

15 Martin, R. S., Roberts, T. J., Mather, T. A. and Pyle, D. M.: The implications of H<sub>2</sub>S and H<sub>2</sub>  
16 stability in high-T mixtures of magmatic and atmospheric gases for the production of  
17 oxidized trace species (e.g., BrO and NO<sub>x</sub>). *Chem. Geol.* 263, 143-150, 2009.

18

19 Martin, R. S., Mather, T. A., Pyle, D. M., Power, M. Allen, A. G., Aiuppa, A., Horwell, C. J.  
20 and Ward E. P. W.: Composition-resolved size distributions of volcanic aerosols in the Mt.  
21 Etna plumes, *Journal of Geophysical Research*, 113, D17211, doi:10.1029/2007JD009648,  
22 2008.

23

24 Martin R.S., Ilyinskaya E., Oppenheimer C., The enigma of reactive nitrogen in volcanic  
25 emissions, *Geochimica et Cosmochimica Acta* 95, 93–105, 2012.

26

27 Mather T.A., Allen A. G., Oppeneheimer C., Pyle D. M., McGonigle A. J. S., Size-Resolved  
28 Characterisation of Soluble Ions in the Particles in the Tropospheric Plume of Masaya

1 Volcano, Nicaragua: Origins and Plume Processing, *Journal of Atmospheric Chemistry* 46:  
2 207–237, 2003.

3

4

5 Mather T.A., Pyle D.M. and Allen A.G.: Volcanic source for fixed nitrogen in the early  
6 Earth's atmosphere, *Geology*; October 2004; v. 32; no. 10; p. 905–908; doi:  
7 10.1130/G20679.1.

8

9 McGonigle A. J. S., Inguaggiato S., Aiuppa A., Hayes A. R. and Oppenheimer C., Accurate  
10 measurement of volcanic SO<sub>2</sub> flux: Determination of plume transport speed and integrated  
11 SO<sub>2</sub> concentration with a single device, *Geochem. Geophys. Geosyst.*, 6, Q02003,  
12 doi:10.1029/2004GC000845.

13

14 Mellouki, A.; Laverdet, G.; Jourdain, J. L.; Poulet, G., Kinetics of the reactions Br + NO<sub>2</sub> +  
15 M and I + NO<sub>2</sub> + M, *Int. J. Chem. Kinet.* 1989, 21, 1161.

16

17 Metrich, N; Rutherford, M J. Low pressure crystallization paths of H<sub>2</sub>O-saturated basaltic-  
18 hawaiitic melts from Mt Etna: Implications for open-system degassing of basaltic volcanoes.  
19 *Geochimica et Cosmochimica Acta*, 62, 7: 1195-1205. 1998.

20

21 Millard G. A., Mather T. A., Pyle D. M., Rose, W. I. and Thornton B.: Halogen emissions  
22 from a small volcanic eruption: Modeling the peak concentrations, dispersion, and  
23 volcanically induced ozone loss in the stratosphere, *Geophysical Research Letters*, 33,  
24 L19815, doi:10.1029/2006GL026959, 2006.

25

26 Oppenheimer, C., Tsanev, V. I., Braban, C. F., Cox, R. A., Adams, J. W., Aiuppa, A.,  
27 Bobrowski, N., Delmelle, P., Barclay, J. and McGonigle, A. J. S.: BrO formation in volcanic  
28 plumes. *Geochim. Cosmochim. Ac.*, 70, 2935-2941, 2006.

29

1 Oppenheimer C., Kyle P. Eisele F., Crawford J., Huey G., Tanner D., Saewung K., Mauldin,  
2 L., Blake, D., Beyersdorf A., Buhr M. and Davis D.: Atmospheric chemistry of an Antarctic  
3 volcanic plume, *J. of Geophys. Res.*, 115, D04303, doi:10.1029/2009JD011910, 2010.  
4

5 Orlando J.J., Burkholder J.B.: Identification of BrONO as the Major Product in the Gas-  
6 Phase Reaction of Br with NO<sub>2</sub>, *J. Phys. Chem. A*, 104, 10, 2048–2053, DOI:  
7 10.1021/jp993713g, 2000.  
8

9 Orlando, J. J., and Tyndall, G. S.: Rate coefficients for the thermal decomposition of BrONO<sub>2</sub>  
10 and the heat of formation of BrONO<sub>2</sub>, *Journal of Physical Chemistry*, 100, 19398-19405,  
11 1996.

12 Rix M., Valks P. Hao N., Loyola D., Schlager H. Huntrieser H., Flemming J., Koehler U.,  
13 Schumann U. and Inness A.: Volcanic SO<sub>2</sub>, BrO and plume height estimations using GOME-  
14 2 satellite measurements during the eruption of Eyjafjallajökull in May 2010, *Journal of*  
15 *Geophysical Research*, 117, D00U19, 19 PP., 1984-2012, DOI: 10.1029/2011JD016718,  
16 2012.  
17

18 Roberts, T. J., Braban, C. F., Martin, R. S., Oppenheimer, C., Adams, J. W., Cox, R. A.,  
19 Jones R. L. and Griffiths., P. T, Modelling reactive halogen formation and ozone depletion in  
20 volcanic plumes. *Chem. Geol.*, 263,151-163, 2009.  
21

22 Roberts T.J., Braban C.F., Martin R.S., Oppenheimer C., Dawson D. H., Griffiths P. T. G,  
23 Cox R.A., Saffell J.R. Jones R.L.: Electrochemical Sensing of Volcanic Plumes, *Chem.*  
24 *Geol., Chemical Geology* 332-333, 74–91, 2012.  
25

26 Roberts T. J., Jourdain L., Griffiths P. T., Pirre M., Re-evaluating the reactive uptake of  
27 HOBr in the troposphere with implications for the marine boundary layer and volcanic  
28 plumes, in review for *ACPD*, 2014.  
29

1 Rose, W. I., Millard G. A., Mather T. A., Hunton D. E., Anderson B., Oppenheimer C.,  
2 Thornton B. F., Gerlach T. M., Viggiano A. A., Kondon Y., Miller T. M., and Ballenthin J.  
3 O.: Atmospheric chemistry of a 33–34 hour old volcanic cloud from Hekla Volcano  
4 (Iceland): Insights from direct sampling and the application of chemical box modeling, *J.*  
5 *Geophys. Res.*, 111, D20206, doi:10.1029/2005JD006872, 2006.

6

7 Satsumabayashi, H., Kawamura M., Katsuno T., Futaki K., Murano K., Carmichael G. R.,  
8 Kajino M., Horiguchi M., and Ueda H.: Effects of Miyake volcanic effluents on airborne  
9 particles and precipitation in central Japan, *J. Geophys. Res.*, 109, D19202,  
10 doi:10.1029/2003JD004204, 2004.

11

12 Scheffler, D., Grothe, H., Willner, A., Frenzel, A., and Zetzsch, C.: Properties of Pure Nitryl  
13 Bromide. Thermal Behavior, UV/Vis and FTIR Spectra, and Photoisomerization to trans-  
14 BrONO in an Argon Matrix, *Inorg. Chem.* 36, 335-338, 1997.

15

16 Schumann U., Weinzierl B., Reitebuch, O. Schlager, H., Minikin A., Forster, C., Baumann  
17 R., Sailer, T., Graf, K., Mannstein, H., Voigt, C., Rahm S., Simmet R., Scheibe, M.,  
18 Lichtenstern, M., Stock, P., Rüba H., Schäuble, D., Tafferner, A., Rautenhaus, M., Gerz T.,  
19 Ziereis, H., Krautstrunk, M., Mallaun, C., Gayet J.-F., Lieke K., Kandler K., Ebert M.,  
20 Weinbruch S., Stohl A., Gasteiger J., Groß S., Freudenthaler V., Wiegner M., Ansmann A.,  
21 Tesche M., Olafsson H., and Sturm K.: Airborne observations of the Eyjafjalla volcano ash  
22 cloud over Europe during air space closure in April and May 2010, *Atmos. Chem.*  
23 *Phys.*, 11, 2245-2279, 2011.

24

25 Simpson W. R., von Glasow R. Riedel K., Anderson P., Ariya P., Bottenheim J., Burrows J.,  
26 Carpenter L. J., Frieß U., Goodsite M. E., Heard D., Hutterli M., Jacobi H.-W., Kaleschke L.,  
27 Neff B., Plane J., Platt, Richter A., Roscoe H., Sander R., Shepson P., Sodeau J., Steffen A.,  
28 Wagner T., and Wolff E., Halogens and their role in polar boundary-layer ozone depletion,  
29 *Atmos. Chem. Phys.*, 7, 4375–4418, 2007.

30

1 Theys N., Van Roozendael M., Dils B., Hendrick, F., Hao, N., and De Mazière M. First  
2 satellite detection of volcanic bromine monoxide emission after the Kasatochi eruption,  
3 *Geophysical Research Letters*, 36, L03809, doi:10.1029/2008GL036552, 2009.

4

5 Vance A., McGonigle, A. J. S., Aiuppa, A., Stith J. L. , Turnbull, K., and von Glasow R.,  
6 Ozone depletion in tropospheric volcanic plumes, *Geophys. Res. Lett.*, 37, L22802,  
7 doi:10.1029/2010GL044997, 2010.

8

9 Voigt, C., P. Jessberger, T. Jurkat, S. Kaufmann, R. Baumann, H. Schlager, N. Bobrowski, G.  
10 Giuffrida, and G. Salerno, Evolution of CO<sub>2</sub>, SO<sub>2</sub>, HCl, and HNO<sub>3</sub> in the volcanic plumes  
11 from Etna, *Geophys. Res. Lett.*, 41, 2196–2203, doi:10.1002/2013GL058974, 2014.

12

13 Von Glasow, R., Bobrowski, N. and Kern, C.: The effects of volcanic eruptions on  
14 atmospheric chemistry, *Chem. Geol.*, 263, 131-142, 2009.

15

16 Von Glasow, R.: Atmospheric Chemistry in Volcanic Plumes, *PNAS*, 107, 15, 6594-6599,  
17 2010.

18

19 Wang, T. X., Kelley, M. D., Cooper, J. N., Beckwith, R. C. and Margerum, D. W:  
20 Equilibrium, kinetic and UV-spectral characteristics of aqueous bromine chloride, bromine  
21 and chlorine species, *Inorg. Chem.*, 33, 5872-5878 , 1994.

- 1 Table 1. Thermodynamic modelling of the high temperature near vent plume using HSC:
- 2 Overview of Inputs and Outputs.

HSC Input: Chemical	Comments
H <sub>2</sub> O, CO <sub>2</sub> , SO <sub>2</sub>	Major Volcanic Gases
HF, HCl, HBr, HI	Halogen Emissions
H <sub>2</sub> S, CO, H <sub>2</sub>	Reduced Gases
Hg	Trace Metals
N <sub>2</sub> , O <sub>2</sub> , Ar	Air

#### HSC Input: Physical

V <sub>A</sub> :V <sub>M</sub>	Atmospheric:Magmatic Gas Ratio
Temperature	Magmatic and Ambient Temperature

#### HSC Output:

Full Matrix of Species	(* see footnote)
------------------------	------------------

#### Key Reactive Species in Output:

NO, OH, Cl, Br, Cl <sub>2</sub>	Species that act to kick-start BrO chemistry
SO <sub>3</sub>	Sulfur trioxide: direct precursor to sulphuric acid H <sub>2</sub> SO <sub>4</sub> (or SO <sub>4</sub> <sup>2-</sup> : Sulfate)

#### Major Volcanic Gases in Output:

SO <sub>2</sub> , HCl, HBr, CO <sub>2</sub> , H <sub>2</sub> O	Present in plume & in HSC output
H <sub>2</sub> S, H <sub>2</sub> , CO	Present in plume but missing in HSC output

3

4 \* Full Matrix of Species typically included in HSC output:

5 H<sub>2</sub>O, N<sub>2</sub>, CO<sub>2</sub>, SO<sub>2</sub>, H<sub>2</sub>, HCl, O<sub>2</sub>, H<sub>2</sub>S, CO, Ar, S<sub>2</sub>, SO<sub>3</sub>, SO, NO, HBr, COS, HS, OH, Cl, Br,  
 6 S<sub>2</sub>O, H<sub>2</sub>S<sub>2</sub>, Cl<sub>2</sub>, I, HOCl, S<sub>3</sub>, HI, HF, H, H<sub>2</sub>SO<sub>4</sub>, BrCl, NO<sub>2</sub>, S, ClO, O, HO<sub>2</sub>, Br<sub>2</sub>, HIO, H<sub>2</sub>O<sub>2</sub>,  
 7 HNO<sub>2</sub>, SOCl, ICl, HCOOH, CS<sub>2</sub>, BrO, S<sub>2</sub>Cl, N<sub>2</sub>O, NOCl, HSO<sub>3</sub>Cl, IBr, SCl, S<sub>4</sub>, IO, NOBr,  
 8 COOH, HNO, NH<sub>3</sub>, ClOO, S<sub>5</sub>, SCl<sub>2</sub>, CH<sub>4</sub>, HNO<sub>3</sub>, HCO, BrOO, CS, OCIO, O<sub>3</sub>, I<sub>2</sub>, ClO<sub>2</sub>,  
 9 SBr<sub>2</sub>, HClCO, SOCl<sub>2</sub>, ClClO, ClOCl, NOI, NO<sub>2</sub>Cl, SO<sub>2</sub>Cl<sub>2</sub>, SOF, IOO, HSO<sub>3</sub>F, ClOCl, SN,

- 1 COCl, NO<sub>3</sub>, S<sub>2</sub>Cl<sub>2</sub>, OBrO, S<sub>6</sub>, F, NBr, HOCN, HNCO, BrOBr, CH<sub>3</sub>, ClF, HCN, COCl<sub>2</sub>,
- 2 N<sub>2</sub>O<sub>2</sub>, BrF, NH<sub>2</sub>, OIO, IF, N, BrBrO, S<sub>2</sub>Br<sub>2</sub>, NOF, IIO, N<sub>2</sub>O<sub>3</sub>, NH<sub>2</sub>OH, SO<sub>2</sub>ClF, SF



1 Table 2. Parameters varied in *PlumeChem* sensitivity studies

Parameter	Values
HSC $V_A:V_M$	0:100 8:92 5:95 10:90 15:85
Aerosol Loading: $\mu\text{m}^2 / \text{molec SO}_2$	
High	$10^{-10}$
Medium	$10^{-11}$
$\text{Br}_{\text{tot}}/\text{SO}_2$ : molar ratio	
Medium	$7.4 \cdot 10^{-4}$
High	$2.4 \cdot 10^{-3}$
Low	$4.8 \cdot 10^{-4}$
Gas Flux kg/s $\text{SO}_2$	
(small variations)	10, 20
(large variations)	10, 50, 100
Wind-speed, m/s	3, 5, 10, 15
Dispersion	B, C, D
Pasquill-Gifford cases	

2

3

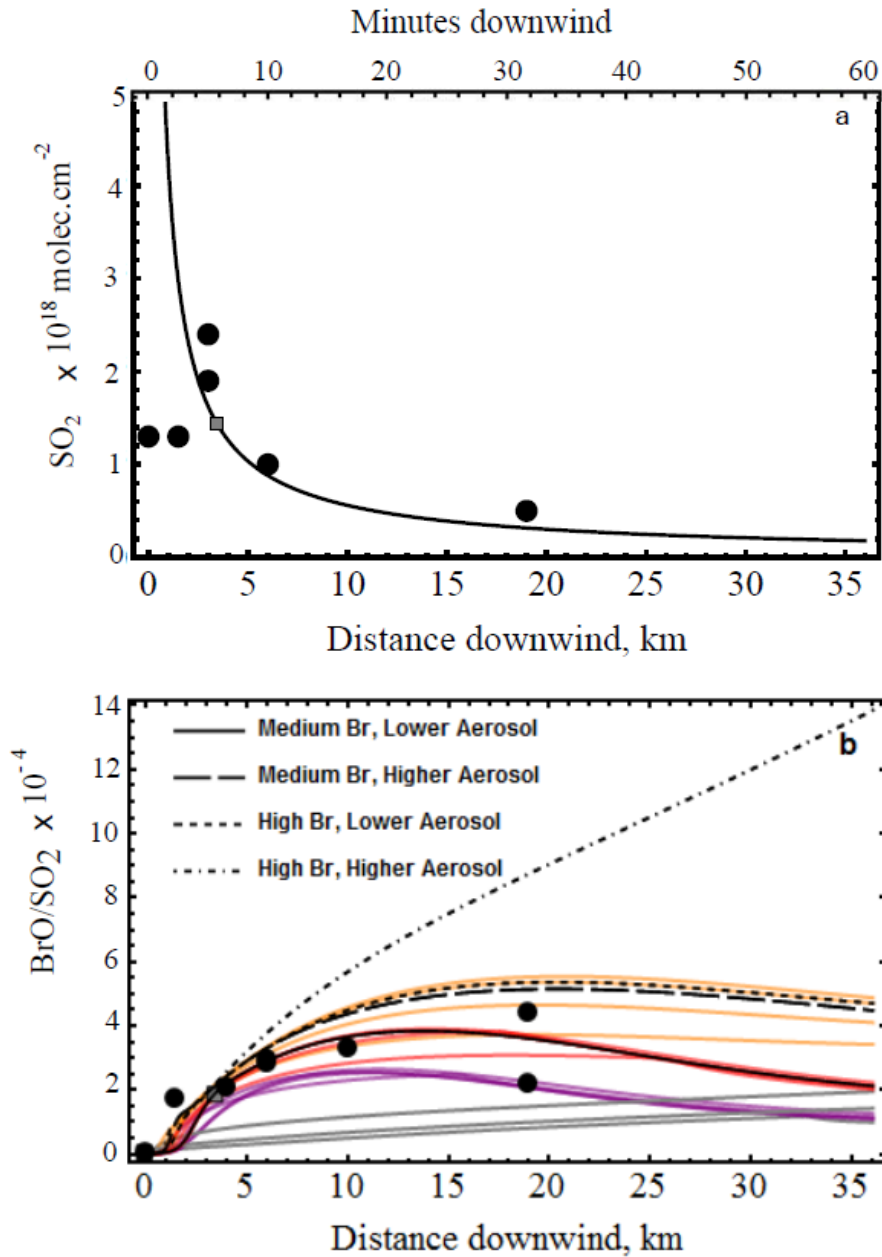
1 Table 3. List of gas-phase and photolytic reactions related to formation of BrNO<sub>2</sub>, BrONO  
 2 and BrNO. Reactions listed are used in the -BrONO-BrNO scheme. The 2-reaction BrNO<sub>2</sub>  
 3 scheme assumes BrNO<sub>2</sub> as the sole product from both Br + NO<sub>2</sub> reactions and photolysis of  
 4 BrNO<sub>2</sub> as the only loss pathway. See text for discussion of possible additional heterogeneous  
 5 pathways.

6

Reaction	Rate Coefficient	at 285 K
$Br + NO_2 \rightarrow BrNO_2$	$\sim 3.8 \times 10^{-13} \text{ cm}^3 \text{ molecule}^{-1} \text{ s}^{-1}$	Brökse et al., 1998
$Br + NO_2 \rightarrow BrONO$	$\sim 4.8 \times 10^{-12} \text{ cm}^3 \text{ molecule}^{-1} \text{ s}^{-1}$	Brökse et al., 1998
$BrONO + Br \rightarrow Br_2 + NO_2$	$2.4 \times 10^{-11} \text{ cm}^3 \text{ molecule}^{-1} \text{ s}^{-1}$	Mellouki et al. 1989
$BrONO + NO_2 \rightarrow BrNO_2 + NO_2$	$\sim 2 \times 10^{-16} \text{ cm}^3 \text{ molecule}^{-1} \text{ s}^{-1}$ (uncertain)	Brökse et al., 1998
$BrONO \rightarrow Br + NO_2$	$\sim 1.2 \text{ s}^{-1}$ (at 298 K, 1 atm) $\tau < 1 \text{ s}$ at 298 K	Brökse et al., 1998 Orlando and Burkholder 2000
$BrONO \rightarrow BrNO_2$	unknown	-
$BrNO_2 + Br \rightarrow Br_2 + NO_2$	unknown	-
$BrNO_2 + NO \rightarrow BrNO + NO_2$	$2.3 \times 10^{-12} \text{ Exp}[-17.8/RT] \text{ cm}^3 \text{ molec}^{-1} \text{ s}^{-1}$	Brökse et al., 1998
$BrNO_2 + NO \rightarrow BrNO + NO_2$	unknown, larger than BrNO <sub>2</sub> equivalent	-
$BrNO + Br \rightarrow Br_2 + NO$	$3.7 \times 10^{-10} \text{ cm}^3 \text{ molecule}^{-1} \text{ s}^{-1}$ or: $5.2 \times 10^{-12} \text{ cm}^3 \text{ molecule}^{-1} \text{ s}^{-1}$	Hippler et al. 1978 Grimley et al. 1980
$BrNO_2 \rightarrow Br + NO_2$	$\leq 4.0 \times 10^{-4} \text{ s}^{-1}$ $\sim 6.4 \times 10^{-5} \text{ s}^{-1}$	Brökse et al., 1998
$2BrNO_2 \rightarrow Br_2 + 2NO_2$	Unknown (slow)	Brökse et al., 1998
$BrONO \xrightarrow{h\nu} Br + NO_2$	$\tau \sim \text{s}$ (products unknown)	Burkholder and Orlando, 2000
$BrONO \xrightarrow{h\nu} BrO + NO$	or $\tau \sim \text{s}$ (products unknown)	
$BrNO_2 \xrightarrow{h\nu} Br + NO_2$	$\tau \sim \text{min}$	Scheffler et al. 1997

7

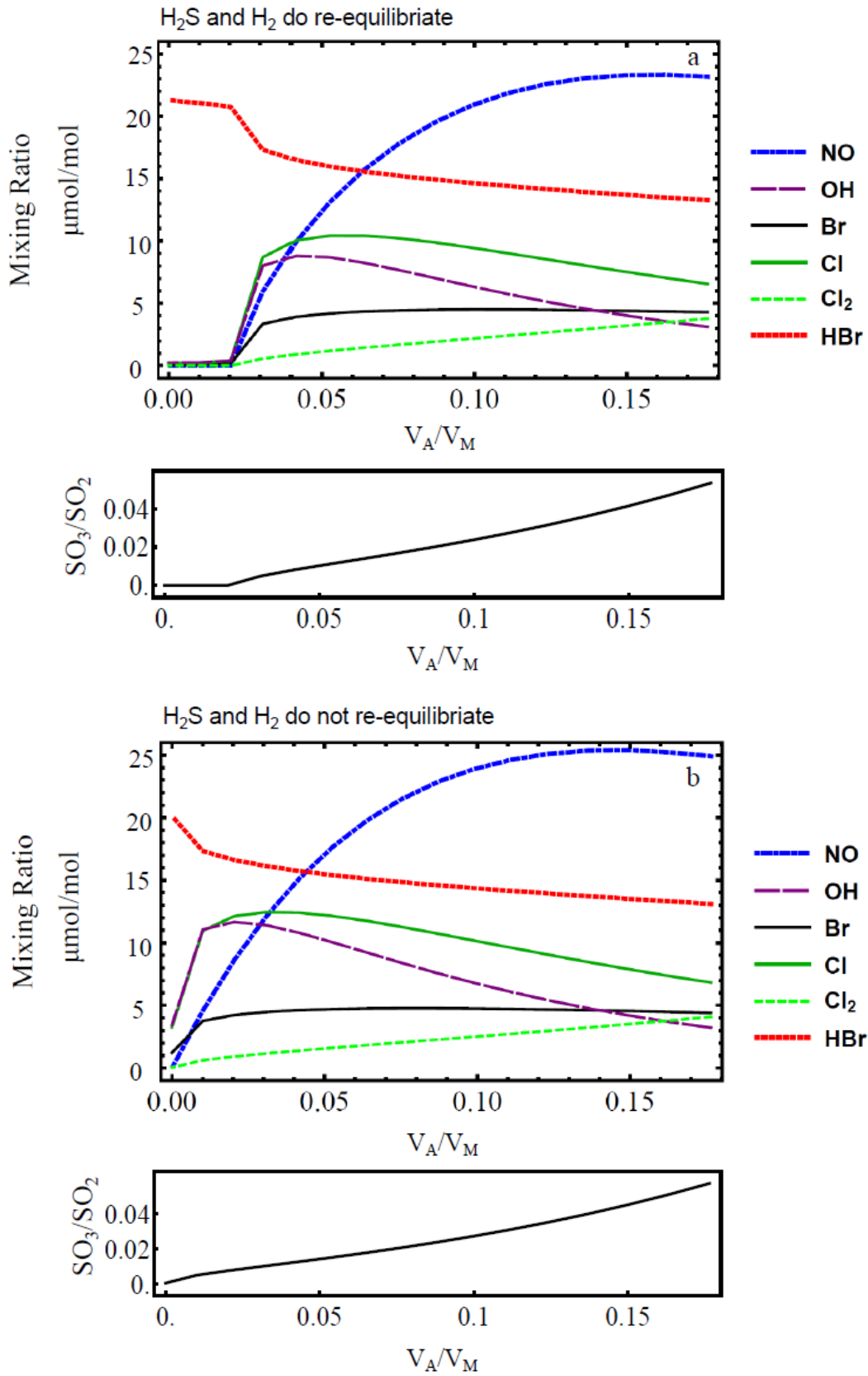
1



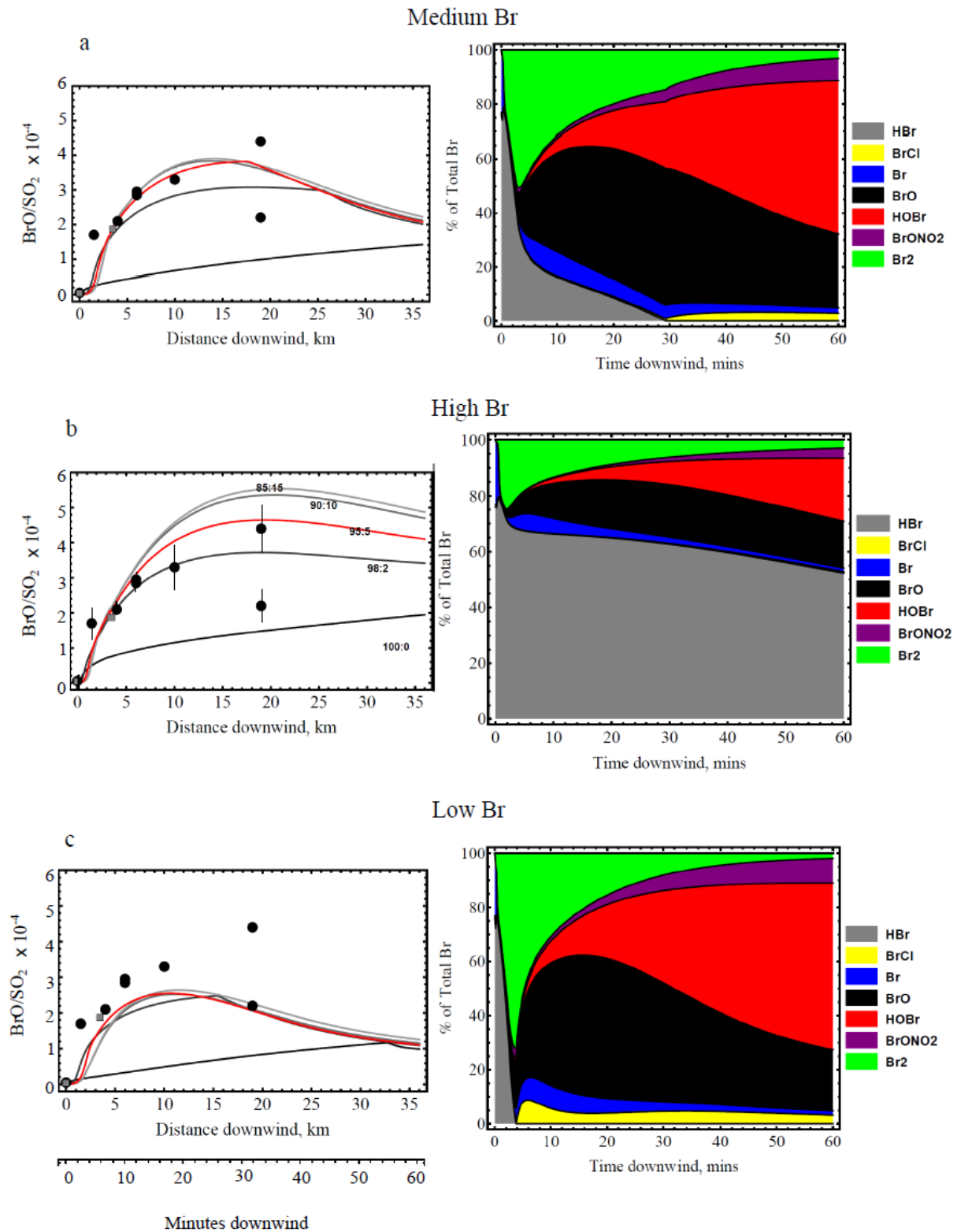
2

3 Figure 1. *PlumeChem* simulations illustrating (a) predicted SO<sub>2</sub> column abundance in the  
 4 downwind plume (black line) according to the model dispersion parameterisation, (b)  
 5 simulated downwind BrO/SO<sub>2</sub> ratios for model runs using this dispersion parameterisation  
 6 but where: bromine in the emission (Br<sub>tot</sub>/SO<sub>2</sub>), volcanic aerosol loading, and the high-  
 7 temperature initialisation are varied. The simulations are compared to DOAS SO<sub>2</sub> column  
 8 abundances and (mean) BrO/SO<sub>2</sub> ratios reported by Oppenheimer et al., (2006), and  
 9 Bobrowski et al., (2007a), gray squares and black disks, respectively. Simulations with

1 varying aerosol emission (for two bromine scenarios) are highlighted in black. Simulations  
2 assuming medium aerosol loading and varying bromine emission (for a range of plausible  
3 high-temperature model initialisations) are shown in red, orange and purple for medium, high  
4 and low Br emission scenarios, respectively. Simulations assuming no plume-air mixing in  
5 the high-temperature initialisation (VA:VM = 0:100) are shown in grey.



1 Figure 2. Mixing ratio ( $10^{-6}$  mol/mol) of key species (NO, OH, Br, Cl, Cl<sub>2</sub>) in the HSC output  
2 as a function of  $V_A/V_M$ , the assumed magmatic: atmospheric gas ratio in the near-vent plume,  
3 ranging from 0 (0.00:1.00) to 0.18 (0.15:0.85). SO<sub>3</sub>:SO<sub>2</sub> ratios (that prescribe the volcanic  
4 sulfate/SO<sub>2</sub> emission) in the HSC output are also shown. (a) Standard operation of HSC in  
5 which volcanic H<sub>2</sub>S and H<sub>2</sub> are allowed to re-equilibrate, yielding near-zero mixing ratios of  
6 these gases in the HSC output. (b) A revised operation of HSC (Martin et al., 2009) in which  
7 volcanic H<sub>2</sub>S and H<sub>2</sub> are removed (and temporarily replaced by inert Ar) such that they do not  
8 re-equilibrate within HSC.



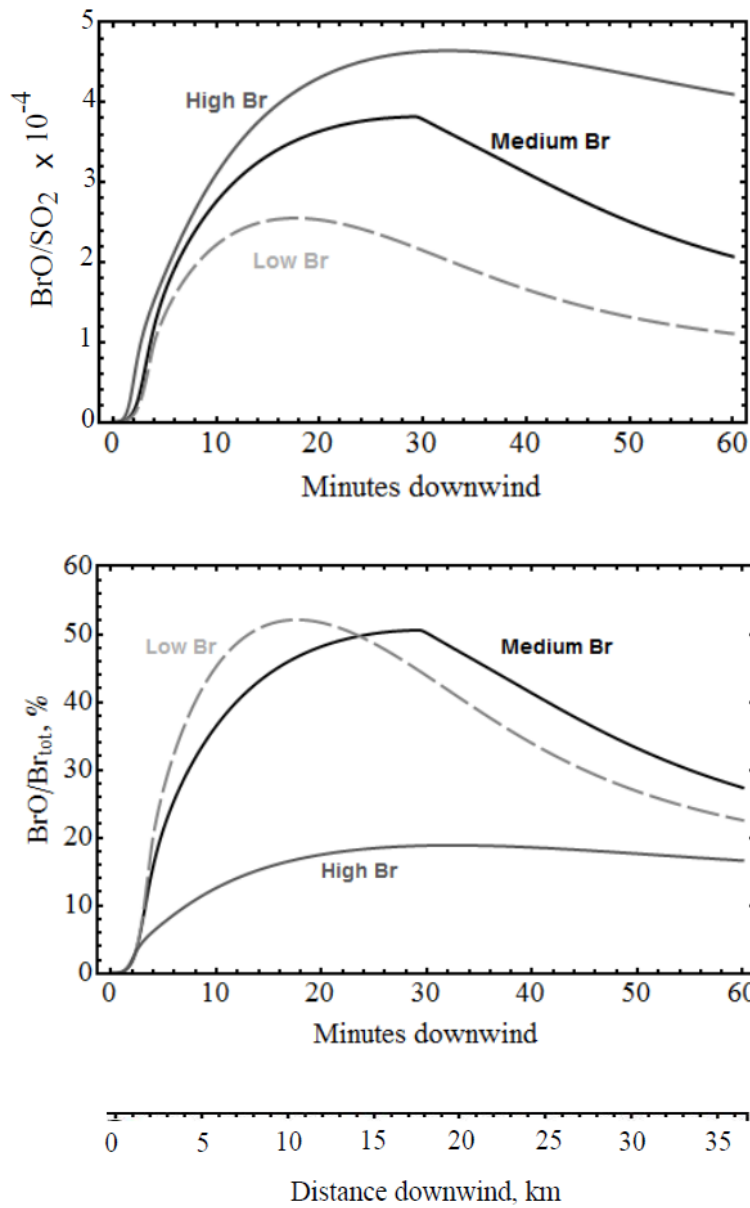
1

2 Figure 3. Left: Simulated 1 hr evolution of plume BrO/SO<sub>2</sub> for the three bromine emission  
 3 scenarios, with varying atmospheric:magmatic gas ratio V<sub>A</sub>:V<sub>M</sub> (0:100, 5:95, 10:90, 15:85) in  
 4 the high-temperature initialisation. Also shown are observed BrO/SO<sub>2</sub> ratios reported by  
 5 Oppenheimer et al., (2006), and Bobrowski et al., (2007a); grey and black disks respectively,

1 with representative data error bars from Bobrowski et al., (2007a). Right: Br-speciation for  
2 the three bromine emission scenarios shown for the model run initialised using HSC with  
3  $V_A:V_M = 5:95$ .  
4



1



2

3 Figure 4. Predicted evolution in  $\text{BrO}/\text{SO}_2$  (top) and  $\text{BrO}/\text{Br}_{\text{tot}}$  ratios (bottom) over 1 hr for the  
4 three different bromine emission scenarios. Model runs correspond to those shown in Figure  
5 3 assuming VA:VM = 5:95 for the high-temperature initialisation.

6

2 reaction scheme ( $\text{BrNO}_2$ )

Improved scheme ( $\text{BrNO}_2$ ,  $\text{BrONO}$ ,  $\text{BrNO}$ )

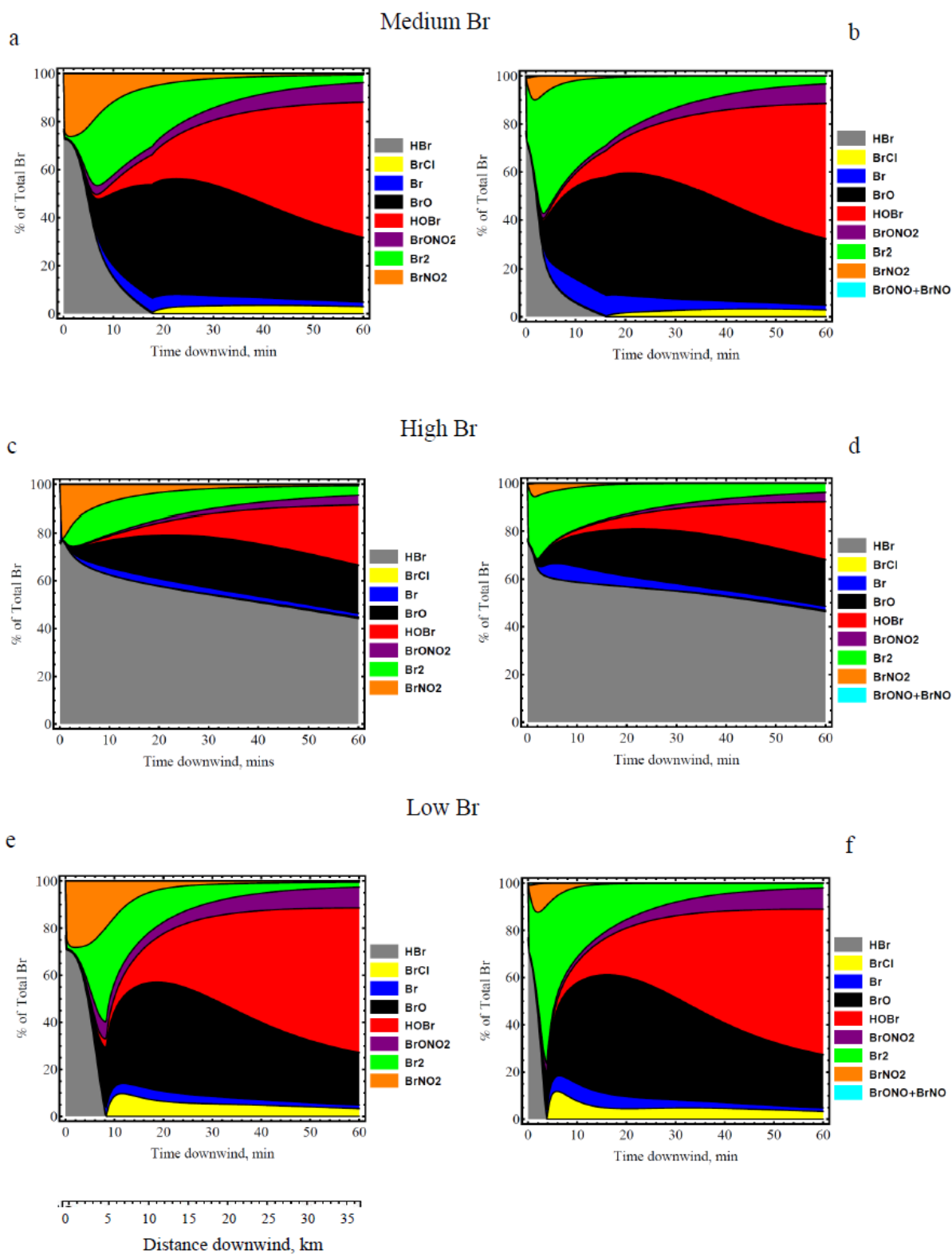
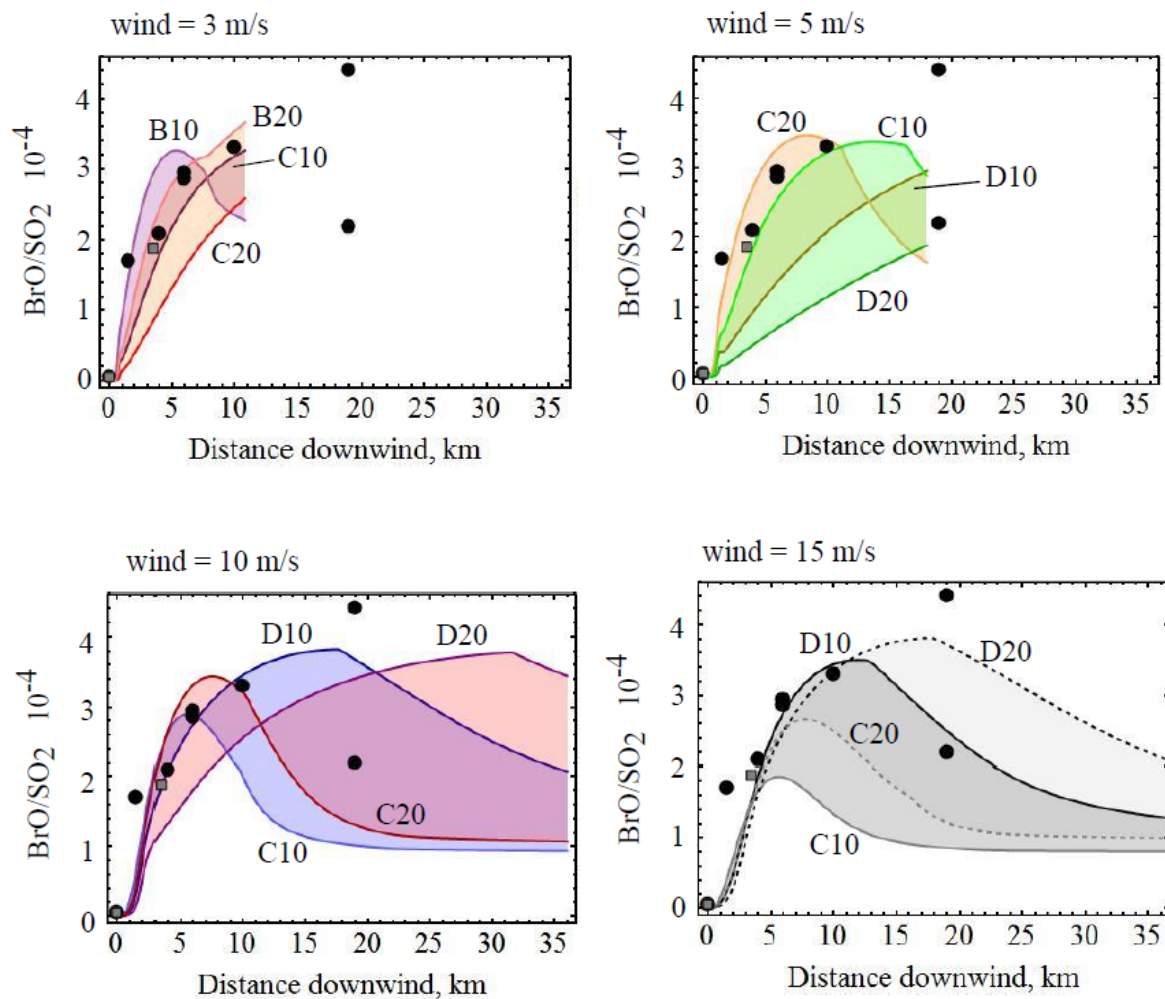


Figure 5. Br-speciation in model runs that also include formation of  $\text{BrNO}_2$ , shown for the three bromine emission scenarios. Simulations incorporate  $\text{BrNO}_2$  using a 2-reaction scheme

- 1 (a,c,e) or a 12-reaction scheme including  $\text{BrNO}_2$ ,  $\text{BrONO}$  and  $\text{BrNO}$  (b,d,f). See text for
- 2 details.

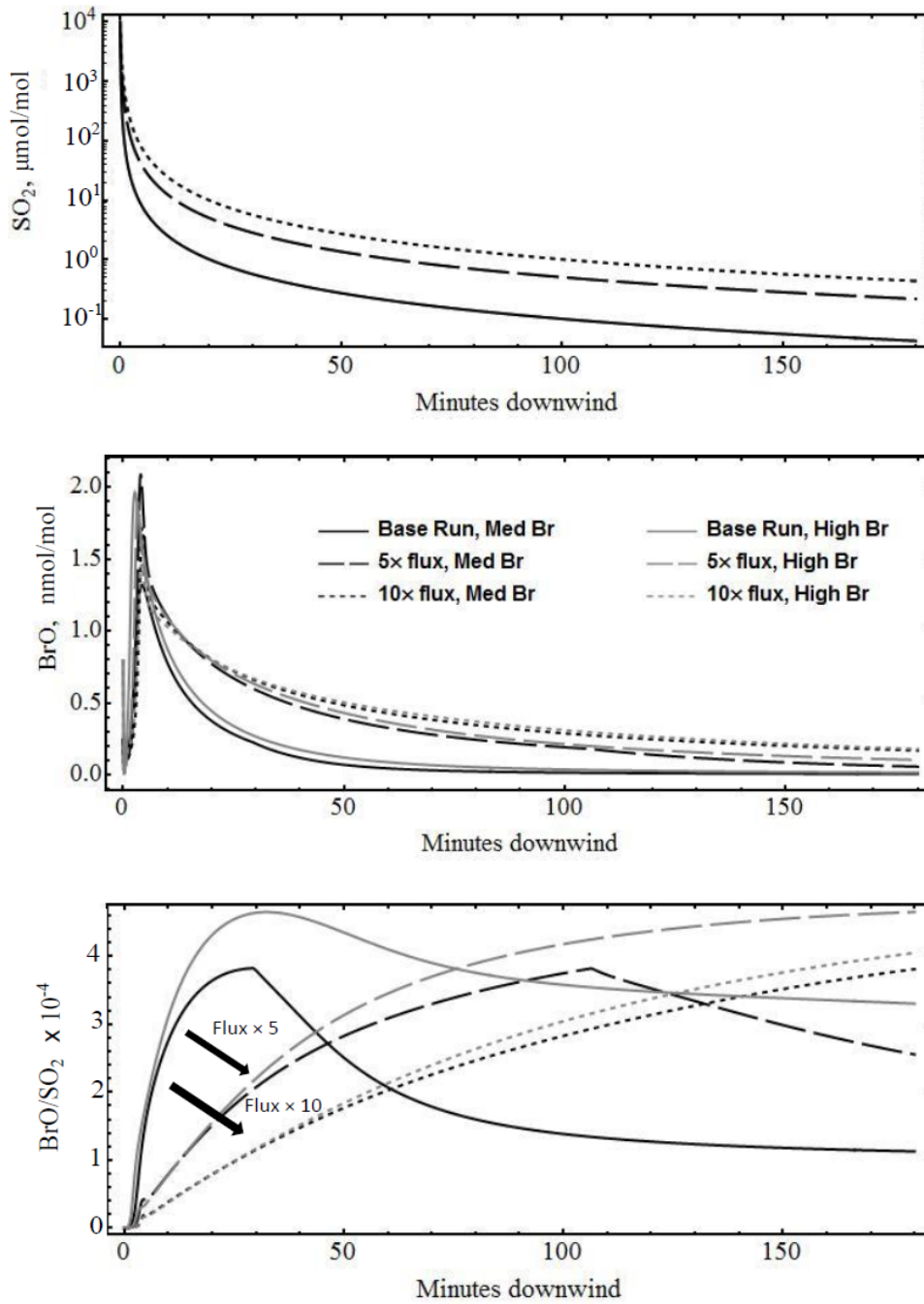


1

2 Figure 6. Simulated BrO/SO<sub>2</sub> over 1 h for the medium bromine emission, predicted for two  
 3 emission flux scenarios (10 or 20 kg/s), and for a range of wind-speeds (3, 5, 10, 15 m/s), and  
 4 Pasquill-Gifford dispersion schemes (B, C, D). See text for details of the combinations.  
 5 Model runs are compared to observations from Bobrowski et al. (2007) and Oppenheimer et  
 6 al. (2006), shown as black circles and grey squares, respectively.

7

1  
2

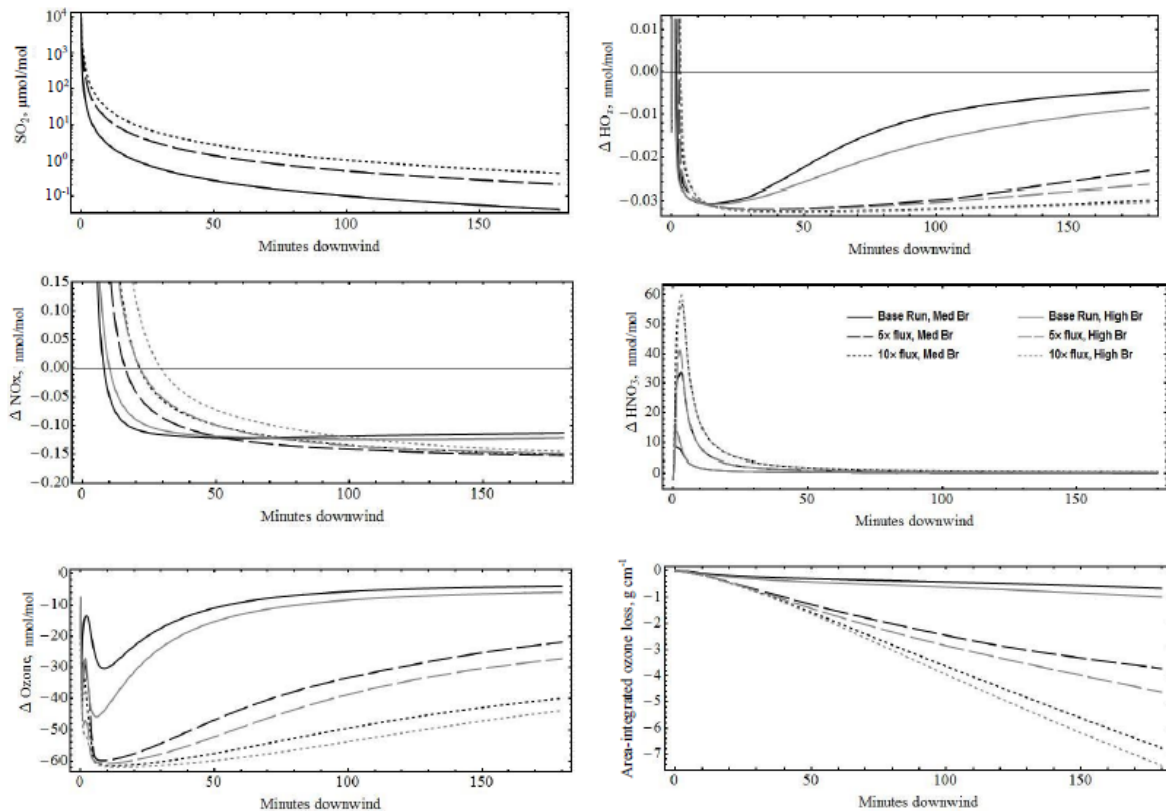


3

4 Figure 7.

5 Simulated plume  $\text{SO}_2$ ,  $\text{BrO}$  and  $\text{BrO}/\text{SO}_2$  over 3 hours for the medium and high bromine  
6 emission scenarios, and with varying volcanic emission flux (baseline run, and with volcanic  
7 gas+aerosol emissions flux  $\times 5$  and  $\times 10$ , shown by full-, long-dashed and short-dashed lines,  
8 respectively), whilst keeping the same plume dispersion parameterisation, wind-speed and

- 1 initialisation (see text for model details and interpretation). Arrows highlight the reduction in
- 2 near-downwind BrO/SO<sub>2</sub> predicted at greater volcanic emission flux.



1  
 2 Figure 8.  
 3 Simulated impact of plume BrO chemistry on atmospheric oxidants, shown for the model  
 4 scenarios of Figure 7. Depletion of oxidants and formation of  $\text{NO}_y$  is shown through the  
 5 difference in plume – background mixing ratio for  $\text{HO}_x$  ( $\text{OH}+\text{HO}_2$ ),  $\text{NO}_x$  ( $\text{NO}+\text{NO}_2$ ),  $\text{HNO}_3$ ,  
 6 and ozone. Cumulative ozone loss is also calculated across the 3 hour simulations.